



HAL
open science

Release-killing properties of a textile modified by a layer-by-layer coating based on two oppositely charged cyclodextrin polyelectrolytes

Jatupol Junthip, Nicolas Tabary, Mickael Maton, Safa Ouerghemmi, Jean-Noel Staelens, Frederic Cazaux, Christel Neut, Nicolas Blanchemain, Bernard Martel

► To cite this version:

Jatupol Junthip, Nicolas Tabary, Mickael Maton, Safa Ouerghemmi, Jean-Noel Staelens, et al.. Release-killing properties of a textile modified by a layer-by-layer coating based on two oppositely charged cyclodextrin polyelectrolytes. *International Journal of Pharmaceutics*, 2020, *International Journal of Pharmaceutics*, 587, pp.119730. 10.1016/j.ijpharm.2020.119730 . hal-02926939

HAL Id: hal-02926939

<https://hal.univ-lille.fr/hal-02926939>

Submitted on 22 Aug 2022

HAL is a multi-disciplinary open access archive for the deposit and dissemination of scientific research documents, whether they are published or not. The documents may come from teaching and research institutions in France or abroad, or from public or private research centers.

L'archive ouverte pluridisciplinaire **HAL**, est destinée au dépôt et à la diffusion de documents scientifiques de niveau recherche, publiés ou non, émanant des établissements d'enseignement et de recherche français ou étrangers, des laboratoires publics ou privés.



Distributed under a Creative Commons Attribution - NonCommercial 4.0 International License

1 **Release-killing properties of a textile modified by a layer-by-layer**
2 **coating based on two oppositely charged cyclodextrin**
3 **polyelectrolytes**

4 *Jatupol Junthip^a, Nicolas Tabary^{a*}, Mickael Maton^b, Safa Ouerghemmi^a, Jean-Noel Staelens^a,*
5 *Frédéric Cazaux^a, Christel Neut^c, Nicolas Blanchemain^b, Bernard Martel^a*

6
7
8 ^a Univ. Lille, CNRS, INRAE, Centrale Lille, UMR 8207 - UMET - Unité Matériaux et
9 Transformations, F-59000 Lille, France

10 ^b INSERM U1008, CHU Lille, Controlled Drug Delivery Systems and Biomaterials, 59000
11 Lille, France

12 ^c INSERM U995 LIRIC, Laboratory of Bacteriology, College of Pharmacy, 59000 Lille,
13 France

14
15 *: Author for correspondence :
16 Dr. Nicolas Tabary
17 Université Lille1
18 Unité Matériaux et Transformations
19 Bâtiment C6, Bureau 119
20 59655 Villeneuve d'Ascq
21 France
22 Tel: 03 20 43 43 30
23 Email: nicolas.tabary@univ-lille.fr

39 **Abstract**

40

41 Infections represent a major medical concern and have severe impact on the public
42 health economy. Antimicrobial coatings represent one major solution and are the subject of
43 many investigations in academic and industrial research. Polyelectrolyte multilayers (PEMs)
44 consist in the step-by-step deposition of polyanions and polycations films on surfaces. The
45 wide range of disposable polyelectrolytes makes this approach among the most versatile
46 methods as it allows to design surfaces that prevent bacterial adhesion, and kill bacteria by
47 contact or by releasing antibacterial agents. The present work focused on the release-killing
48 effect of an active PEM coating of a polyethylene terephthalate (PET) textile support. This
49 activity was obtained thanks to the PEM film build up using cationic and anionic
50 polyelectrolytes both based on cyclodextrins (PCD- and PCD+) that provided a reservoir
51 property and prolonged release of triclosan (TCS). To this effect, a PET non-woven
52 preliminarily modified with carboxylate groups by applying a thermofixation process was
53 then treated by dip-coating, alternating soaking cycles in cationic PCD+ and in anionic PCD-
54 solutions. Samples coated with such PEM film were then loaded with TCS whose release was
55 assessed in dynamic mode in a phosphate buffered saline solution (PBS) at 37°C. In parallel,
56 TCS/PCD+ and TCS/PCD- interactions were investigated by Nuclear Magnetic Resonance
57 (NMR) and phase solubility study, and the biocide activity was assessed against *S. aureus* and
58 *E. coli*. Finally, the present study has demonstrated that our PCD+/PCD- PEM system
59 presented release-killing properties that supplement the contact-killing effect of this system
60 that was reported in a previous paper.

61

62

63

64 **Keywords:** β -cyclodextrin polymers, polyelectrolytes multilayer (PEM), textile, drug
65 delivery system, antibacterial textile.

66 1. Introduction

67 Infections represent a major medical concern and has severe impact on the public
68 health economy. Antimicrobial coatings of medical devices and implants is one major
69 solution and is the subject of many investigations in academic and industrial research.
70 Polyelectrolyte multilayers (PEMs) introduced by Decher *et al.* in 1992 (Decher et al., 1992)
71 consist in the step-by-step deposition of polyanions and polycations building layer-by layer
72 (LbL) films on surfaces. The wide range of disposable polyelectrolytes makes this approach
73 among the most versatile methods for the design of antibacterial surfaces as PEMs present the
74 great advantages (i) to be applicable to a large variety of substrates (Boudou et al., 2010;
75 Hammond, 2012), (ii) to be tunable in terms of chemical, physicochemical and mechanical
76 properties (Phelps et al., 2011) and iii) to embed and release a wide range of antimicrobial
77 compounds. Three general strategies are commonly used in the design of LbL antimicrobial
78 films (Lichter et al., 2009; Lichter and Rubner, 2009; Séon et al., 2015). The first approach
79 consists in the prevention of the bacterial adhesion through the adjustment of the surface
80 hydrophobicity (Chen et al., 2010; Genzer and Efimenko, 2006), the surface charge (Zhu et
81 al., 2015) or the surface stiffness (Lichter et al., 2008). The second approach is based on
82 contact-killing surfaces obtained by the immobilization into the LbL film of polymers
83 carrying cationic groups. Antimicrobial peptides, synthetic polymers carrying amine groups
84 such as polyallylamine (Lichter and Rubner, 2009), quaternary ammonium salts such as
85 poly(diallyldimethylammonium chloride) (Zhu et al., 2015), chitosan biopolymer (Wang et
86 al., 2012) and its quaternary ammonium derivatives (Graisuwan et al., 2012) are the most
87 commonly used solutions (Lichter et al., 2009; Zhu and Loh, 2015). The third approach
88 consists in the release of antimicrobial agents compound toward the tissues directly in contact

89 with the implant or the device such as copper or silver salts or nanoparticles (Dai and
90 Bruening, 2002), antibiotics especially cationic ones such as gentamicin (Chuang et al., 2008),
91 antimicrobial peptides (Shukla et al., 2010), nitric oxide (Cai et al., 2011), antiseptic agents
92 (Agarwal et al., 2012; Nguyen et al., 2007; Séon et al., 2015; Wang et al., 2014) (triclosan,
93 chlorhexidine) have been especially studied. Concerning the two later strategies, it is worth to
94 mention that the antibacterial effect of contact killing surfaces often lasts longer than release
95 based coatings since the LbL film degradation is in general slower than the release
96 phenomenon.

97 Recently, our group successfully developed contact-killing PEMs films based on the one
98 hand on cationic β -cyclodextrin polymers crosslinked with epichlorohydrin in the presence of
99 glycidyl trimethylammonium chloride (PCD+), and on the other hand on an anionic β -
100 cyclodextrin polymer crosslinked with citric acid (polyCTR-CD = PCD-). Such LbL system
101 was built onto a nonwoven PET textile whose surface was preliminarily modified with
102 carboxylic acid groups in order to provide the requested anionic character to the support
103 (Junthip et al., 2015). Thanks to their high glycidyl trimethylammonium chloride content,
104 such LbL systems presented a relevant intrinsic bacterial reduction up to 7.3 log against *S.*
105 *aureus* and 4.5 log against *E. coli* (Junthip et al., 2016).

106 In the present work, the contact-killing PCD+/PCD- LbL system described above was
107 loaded with triclosan (TCS), a broad-spectrum antimicrobial agent (Jones et al., 2000;
108 Yazdankhah et al., 2006) commonly used in personal care products (Cheng et al., 2011) that
109 conveniently exhibits a high host-guest complexation affinity with cyclodextrins (Duan et al.,
110 2005; Loftsson et al., 1999; Lu et al., 2001). Thereby, a dual antimicrobial action system was
111 expected, combining the contact-killing effect provided by the trimethylammonium groups of
112 PCD+ on the one hand, and the release-killing effect obtained TCS release on the other hand
113 (Figure 1). **To our knowledge, only a few dual release and contact killing LbL systems with**

114 multiple bactericidal components have been already described in the literature (Zhu and Loh,
115 2015). Despite PEM integrating CDs have been particularly studied in drug delivery (Fagui et
116 al., 2014; Leguen et al., 2007; Smith et al., 2009) and in biomaterials applications (Benkirane-
117 Jessel et al., 2004; Chen et al., 2011; Martin et al., 2013a; Teo et al., 2015), the only existing
118 work dealing with the concept of dual functionality was reported by Wong et al. who prepared
119 a dual functional PEM coating including a poly(carboxymethylcyclodextrin) and N,N-
120 dodecyl,methyl-polyethyleneimine that displayed both prolonged release of anti-inflammatory
121 diclofenac and contact microbiocidal activity (Wong et al., 2010).

122 To achieve our objective, a nonwoven PET coated with an LbL film made of five
123 PCD+/PCD- bilayers was prepared and characterized by Scanning Electron Microscopy
124 (SEM). The release-killing effect was obtained by loading TCS on samples, whose release
125 kinetics was performed in phosphate buffered saline (PBS) at 37°C in a dynamic system. TCS
126 inclusion in CD cavities present in both PCD+ and PCD- were investigated by proton Nuclear
127 Magnetic Resonance (NMR) and by phase solubility study. The antibacterial activities of the
128 samples loaded with TCS dipped in PBS medium over a period of 28 days were assessed in
129 parallel by diffusion test.

130

131 **2. Materials & Methods**

132 **2.1. Materials**

133 β CD was a gift from Roquette (Kleptose®, Lestrem, France).
134 Glycidyltrimethylammonium chloride (GTMAC), epichlorohydrin (EP), sodium dihydrogen
135 hypophosphite ($\text{NaH}_2\text{PO}_2 \cdot \text{H}_2\text{O}$), sodium hydroxide (NaOH), citric acid (CTR), triclosan
136 (TCS), phosphate buffered saline (PBS, for solution 0.15 M at pH=7.4) and potassium
137 dihydrogen phosphate (for solution 50 mM at pH=6.5) were supplied from Sigma Aldrich
138 (Saint-Quentin Fallavier, France).

139 The textile support was a polyethylene terephthalate non-woven (PET, thickness =
140 0.24 mm, surface weight = 65 g/m², reference NSN 365) donated by PGI-Nordlys (Bailleul,
141 France).

142 Anionic water-soluble polymer of β -cyclodextrin (polyCTR-CD or PCD-) was
143 prepared according to a method described by Martel et al. (Martel et al., 2005) by the
144 solubilization of β -cyclodextrin, sodium hypophosphite as catalyst and citric acid as
145 crosslinking agent in respective weight ratio 10g/ 3g/ 10g in 100 mL of water. After water
146 removal by rotary evaporator, the resulting solid mixture was then cured at 140°C during 30
147 min under vacuum. After water addition, the resulting suspension was filtered and the filtrate
148 dialyzed during 72 hours against water using 6–8 kDa membranes (SPECTRAPOR 1,
149 Spectrumlabs). Finally, the polyCTR-CD was recovered by freeze drying. Molecular masses
150 in number (Mn) and in weight (Mw), measured by aqueous size exclusion chromatography
151 (SEC) in water equipped with a light scattering detector, were 13.0 kg/mol and 22.6 kg/mol
152 respectively (PDI = 1.7). The charge density of PolyCTR-CD (or COOH groups content) was
153 4 mmol per gram (measured by acid-base titration). The weight composition determined by
154 ¹H NMR was 50 wt.% in CD moieties and 50 wt.% in citrate cross-links.

155 Cationic water-soluble polymer of β -cyclodextrin (polyEPG-CD-10 or PCD+) was
156 synthesized by reacting β CD with epichlorohydrin (EP) in the presence of
157 glycidyltrimethylammonium chloride (GTMAC), with a molar ratio GTMAC/ β CD = 10,
158 under basic conditions as previously described (Junthip et al., 2015). Briefly 5g (4.4 mmol) of
159 β CD was dissolved in 8 mL of NaOH (22% (w/v)) aqueous solution and left under
160 mechanical stirring overnight at room temperature. Then, 7.40 mL (44 mmol) of GTMAC
161 (90%(w/v) in water) and 3.45 mL (44 mmol) of EP were rapidly added to solution heated to
162 60°C during 3 hours before adding acetone. The aqueous phase was heated to 50°C overnight,
163 neutralized with HCl (6 N), dialyzed (cut-off of 6–8 kDa, SPECTRAPOR 1, Spectrumlabs)

164 and finally freeze-dried before collecting polyEPG-CD samples as white powders. Mn and
165 Mw, measured by aqueous size exclusion chromatography (SEC), were 16.1 kg/mol and 25.8
166 kg/mol respectively (PDI = 1.6). The charge density (or trimethylammonium groups content)
167 of polyEPG-CD-10 was 2 mmol/g of polymer (measured by colloidal titration). The weight
168 composition determined by ¹H NMR, was 58 wt.% in CD moieties, 16wt.% in EP cross-links
169 and 26 wt.% in GTMAC.

170

171 **2.2.Layer by Layer coating of the PET textile**

172 The virgin textile PET sample was preliminary functionalized by thermofixation using
173 the *pad-dry-cure* process in order to obtain the negative charges provided by the resulting
174 carboxylic groups strongly anchored on the surface (Martin et al., 2013a, 2013b). Virgin
175 textiles (3 x 3cm²) were impregnated in 100 mL of solution containing β-cyclodextrin (10 g),
176 sodium hypophosphite as catalyst (3 g) and citric acid as crosslinking agent (10 g). The textile
177 was then roll-padded (BHVP model, Roaches, UK) and cured at 150°C in a ventilated oven
178 (Minithermo, Roaches, UK). Samples were finally washed by soxhlet with water. This
179 thermofixation treatment yielded samples provoked a 20wt.% weight gain of the samples
180 (abbreviated PET20) measured with a precision balance ($\pm 4 \cdot 10^{-4}$ g, Precisa 240A),
181 corresponded to a surface density of 6.5 μmol COO⁻/cm² measured by using the calcium
182 acetate titration method (Ducoroy et al., 2008).

183 The LbL build-up was carried out at room temperature by dipping process with both
184 CD cationic and anionic polyelectrolytes solutions (4 g/L) in water at their natural pH, i.e 3.5
185 ± 0.1 (polyCTR-CD) and 6.5 ± 0.2 (polyEPG-CD-10) (Junthip et al., 2015). The thermofixed
186 PET20 samples were firstly dipped during 15 minutes in 50 mL of cationic polymer solution
187 PCD+, drying at 90°C for 15 minutes, rinsing again with 50 mL of distilled water for 15
188 minutes and drying at 90°C for 15 minutes. The similar sequence was then applied with the

189 anionic polymer solution PCD-. Both steps were repeated 4 times to obtain ten self-assembled
190 layers, or five PCD+/PCD- bilayers onto the thermofixed PET supports (abbreviated PET20-
191 PEM5) with a weight gain of $75\% \pm 3\%$ (Junthip et al., 2016).

192 Finally, a thermal treatment of textiles was applied at 140°C in a ventilated oven
193 (MEMMERT, DIN 40050- IP20) for 8 hours in order to improve the PEM film stability in
194 contact with PBS medium.

195

196 **2.3. Triclosan adsorption**

197 The incorporation of TCS was performed by dipping the PET20 and PET20-PEM5
198 samples into 15 mL of a saturated TCS solution during 24 hours under stirring 150 rpm at
199 37°C . Then, samples were washed in 15 mL of distilled water during 5 minutes for three
200 times before drying at 45°C .

201 **2.4. Scanning Electron Microscopy (SEM)**

202 Textile samples were characterized by SEM apparatus SEM instrument (Hitachi S-
203 4700 SEM FEG (Field Emission Gun)), using an acceleration voltage of 5 kV. Textile
204 samples were covered with a carbon layer before their analysis.

205

206 **2.5. Triclosan release study**

207 Drug release was measured with a fully automated flow-through cell dissolution
208 apparatus (Sotax USP4, CE 7 Smart with CP7 piston pump, Switzerland) in a closed loop
209 configuration combined with a UV-visible spectrometer (Perkin Elmer LAMBDA 25). Textile
210 samples containing TCS (100 mg) were placed inside a cylinder flow cell (22.6 mm). The
211 dissolution medium (filtered solution of PBS 0.15 M at $\text{pH}=7.4$) under stirring (200 rpm) was
212 circulated by pumping it through each cell at a rate of 50 mL/min and the temperature was
213 maintained at $37 \pm 0.5^{\circ}\text{C}$ during testing. The concentration of TCS was measured at time

214 intervals and calculated at each time point based on calibration curves (specific extinction
215 coefficient of TCS in PBS at $\lambda=282$ nm was $0.0149 \text{ L mg}^{-1} \text{ cm}^{-1}$ with $r^2=0.9974$).

216

217 **2.6. Complexation study of triclosan with PCD+ and PCD-**

218 **2.6.1. Proton Nuclear Magnetic Resonance**

219 The one and two dimensional ^1H NMR spectra were recorded in D_2O using a Bruker
220 AV 300 spectrometer at 300 MHz with 8 increments for polymers and complexed
221 TCS/polymers, except for TCS with 13056 increments. Two-dimensional NOESY (Nuclear
222 Overhauser Effect Spectroscopy) experiments were operated at 300 K using the standard
223 Bruker parameters and a spin-lock mixing time of 350 ms with TPPI method. 2D spectrum
224 consisted of a matrix of 2048 (F2) by 2048 (F1) covering a sweep width of 1929 Hz and 16
225 increments were collected with 256 transients. A concentrated polymer solution was prepared
226 (50mM) in D_2O before TCS addition in excess, and then it was maintained under agitation
227 (150 rpm) 24 hours at 25°C . The supernatant was characterized by NMR.

228

229 **2.6.2. Phase solubility of TCS with PCD+ and PCD-**

230 Phase solubility of TCS in phosphate buffer (50 mM, pH 6.5) was carried out by
231 adding an excess amount (5mg/mL) of TCS to 10 ml of polymer solution (0 to 8%(w/v)) and
232 βCD solution (0 to 1.6%(w/v)). The mixtures were mechanically shaken at 25°C for 24 hours
233 (until equilibrium), centrifuged and the TCS concentration in the supernatant was determined
234 by UV-visible spectroscopy (Shimadzu UV-1800) at 282 nm. Each experiment was
235 performed in duplicate. In the case of the formation of a 1:1 inclusion complex, the stability
236 constant $K_{1:1}$ was obtained from the equation described by Higuchi and Connors (Higuchi and
237 Connors, 1965) :

238

$$K_{1:1} = \text{Slope} / (S_0 (1-\text{Slope}))$$

239 where S_0 represents the intrinsic solubility of TCS in PBS, and the molar concentration of CD
240 polymers was calculated by considering that β -CD represented 58. wt % and 50. wt % in
241 PCD+ and PCD- respectively.

242

243 **2.7. Antibacterial tests**

244 The diffusion test was applied to evaluate the antimicrobial activity through the
245 measurement of the inhibition zone around the samples put on agar gel seeded with
246 *Staphylococcus aureus*, CIP224 and *Escherichia coli*, K12. The textile samples of 11 mm
247 diameter were sterilized with absolute ethanol during 1 minute before air-drying and then
248 placed in a 24 well plate containing 1 mL of PBS sterilized solution (0.15 M, pH=7.4) under
249 stirring (150 rpm) at 37°C. At the predetermined time points, the PBS solution of each well
250 plate was removed and refilled with a new PBS solution, except at zero time. 100 μ L of the
251 bacterial suspension (1×10^4 colony forming unit (CFU)·mL⁻¹) were then plated on Müller-
252 Hinton-Agar (MHA). Then, the textile samples were deposited on MHA and were incubated
253 at 37°C during 24 hours. Inhibition zone radius (in cm) were measured and plotted as a
254 function of the release time in PBS. The tests were repeated three times to obtain an average
255 value.

256

257 **3. Results & Discussion**

258 **3.1. LbL film build-up onto PET20 samples**

259 LbL deposition of cationic polyEPG-CD-10 and anionic polyCTR-CD onto the
260 nonwoven PET textile were realized as reported previously (Junthip et al., 2016, 2015). After
261 the thermofixation step, textile samples underwent a weight gain of 20%wt and after the
262 superimposition of five PCD+/PCD- bilayers, the weight gain increased up to 75%wt (Junthip
263 et al., 2016). Micrographs displayed in Figure 2 show the evolution of the fibrous support

264 morphology at the fibers scale before treatment, after thermofixation (PET20 sample) and
265 after the ten cycles of the dip coating process (PET20-PEM5). Both modification steps
266 involved an increase of the diameter of the fibers synonym of their coating firstly by the
267 thermofixed layer and then by the LbL film. In the latter case, ~~one can observe that~~ the textile
268 structure was covered by the PEM coating, especially when focusing on the fibers crossings
269 where fibers are bridged together. From this observation, ~~one can notice~~ a decrease of the
270 ~~textile~~ porous volume ~~of the textile, and one can a~~ could also explain the stiffness increase
271 noted upon samples handling, especially ~~observed~~ after the LbL process and the final thermal
272 post-treatment at 140°C.

273

274 **3.2. Study of the complexation of TCS with PCD+ and PCD- by NMR**

275 TCS/polyEPG-CD-10 and TCS/polyCTR-CD interactions were investigated by
276 Nuclear Magnetic Resonance (NMR). In Figure 3.a and 3.b the main signals in both
277 cationic and anionic poly-cyclodextrins spectra could be attributed according to previous
278 reports (Martin et al., 2013b) and (Junthip et al., 2016, 2015). ~~Spectrum in figure 3.a~~
279 ~~relative to polyCTR-CD displayed the signal of the glucopyranosic units of cyclodextrins,~~
280 ~~H1 at 5 ppm, H3, H5, H6, H4 and H2 situated between 3.5 and 4 ppm, the methylene~~
281 ~~groups of the citrate crosslinks appearing between 2.7 and 3 ppm. Finally, two singlets at~~
282 ~~6.25 and 7.8 ppm corresponding to cis and trans aconitic esters respectively issued from a~~
283 ~~side reaction consisting of the dehydration of citrate crosslinks. Spectrum in figure 3.b~~
284 ~~relative to polyEPG-CD-10 displayed the signal of anomeric proton (H-1) of cyclodextrin~~
285 ~~near 5 ppm, the protons of quaternary ammonium of GTMAC at 3.2 ppm and the rest of~~
286 ~~cyclodextrin protons and reactant protons (GTMAC and EP) in the range 3.2 to 4.5 ppm.~~
287 In the presence of TCS, no signal shifts of H3 and H5 cyclodextrins protons could be
288 observed in the 3.7 to 3.9 ppm interval. However, the spectrum magnification reported in
289 Figure 3c displays spectral changes in the range from 6 to 8 ppm where aromatic protons

290 of TCS are situated (Jug et al., 2011; Qian et al., 2008). All aromatic protons of TCS
291 shifted upfield or downfield (Figure 3c), in the presence of both polymers, revealing a
292 possible complexation. This was confirmed by 2D-NOESY NMR spectra (Figure S1)
293 where correlation peaks appeared consequently to the dipolar interaction between the TCS
294 aromatic protons (6 to 8 ppm) with internal proton H3 and H5 of poly-cyclodextrins
295 (around 3.8 to 3.9 ppm).

296

297 **3.3.Phase solubility study of TCS in the presence of PCD+ and PCD-**

298 Solubility enhancement studies of TCS in the presence of β CD, polyCTR-CD and
299 polyEPG-CD-10 were carried out using the phase solubility method (Figure 4). TCS
300 presented intrinsic solubility of 0.04 mM at 25°C that sharply increased by factors up to 10,
301 60 and 220 in the presence of β CD, polyCTR-CD and polyEPG-CD-10, respectively. More
302 specifically, Figure 4a shows an increase in TCS solubility in function of the β CD
303 concentration up to 4.4 mmol/L, and then levels around 0.4 mmol/L. This is typical of a B-
304 type phase-solubility profile (Higuchi and Connors, 1965) indicating the formation of
305 complexes with limited solubility in the aqueous medium. The apparent association constant
306 calculated from the slope of the plot ($K_{1:1}$) was equal to 1870 M⁻¹, in accordance with the
307 literature in which $K_{1:1}$ was equal to 2526 M⁻¹ for the complex β CD: TCS (Jug et al., 2011).
308 TCS solubility linearly increases with both β CD polymers types concentration, displaying in
309 both cases A_L-type profiles (Figure 4b and 4c). The calculated association constants of TCS
310 with polyEPG-CD-10 and polyCTR-CD were equal to 6650 and 1590 M⁻¹ respectively.
311 Elsewhere, the $K_{1:1}$ value of TCS with another type of cationic β CD polymer using choline
312 chloride as cationizing agent was found to be equal to 3800 M⁻¹ in water (Qian et al., 2008).
313 So, this study confirmed that both PCD+ and PCD- can form inclusion complexes with TCS.

314

315 **3.3.1. TCS Release study**

316 PET 20 and PET20-PEM5 samples were loaded with TCS and their release profile were
317 assessed in PBS at 37°C and in dynamic mode at the flow rate of 50mL/min. Figure 5 shows
318 a meaningful influence of the mode of functionalization on the release patterns. As a matter of
319 fact, 4.6 mg of TCS /g of sample were loaded and then released by the textiles modified by
320 thermofixation and then with five self-assembled bilayers, while samples that only underwent
321 the thermofixation step adsorbed and then released only 1.1 mg/g. This result demonstrated
322 that the multilayer film increased of a 3.5 factor the reservoir capacity of the textile. This
323 result can be attributed to the inclusion complex formed between TCS and CD moieties
324 present in both PCD+ and PCD- in the PEM coating.

325 **3.4. Antibacterial activity of samples**

326 PET20 and PET20-PEM5 samples cut in 11mm disks and then loaded with TCS were put
327 in PBS batch at pH 7.4 at 37°C over a period of 28 days. The disks were withdrawn at
328 different time points from the batches and deposited on agar plates pre-inoculated with *S.*
329 *aureus* and *E. coli* (Figure 6a). After 24 hours of incubation, their residual antibacterial
330 activities were reported by plotting the inhibition diameters of halos appearing around
331 samples against the release time in PBS (Figure 6b and 6c). Despite TCS is a broad-spectrum
332 antimicrobial agent, all test samples displayed larger inhibition diameters in the presence of *S.*
333 *aureus* (minimum inhibitory concentration (MIC) of 0.025-1 mg/L) compared to *E. Coli* K12
334 (MIC of 1mg/L), due to the higher sensitivity of Gram+ toward TCS (Assadian et al., 2011;
335 Suller and Russell, 2000). On the other hand, inhibition diameters formed around PET20-
336 PEM5 samples were sharply superior to those observed around PET20 samples loaded with
337 TCS. This can be correlated with the kinetic study that showed that the release rates of TCS
338 from PET20-PEM5 samples were sharply superior compared to PET20 samples. In the course
339 of time of the batch experiments, PET20 samples displayed a fast loss of their antibacterial

340 activity against *E. coli* within 3 days as the inhibition diameters decreased from 2.3 cm to 1.1
341 cm (corresponding to the diameter of disks) within this period. On the contrary, the
342 antibacterial activity of PET20-PEM5 samples against *E. coli* only slightly decreased during
343 the 28 days period as inhibition diameters decreased from 3.1 cm down to 2.7 cm. Besides,
344 PET20 and PET20-PEM5 samples displayed a sustained antibacterial effect even after 28
345 days against *S. aureus*. However, the antibacterial activity of PET20 samples against *S.*
346 *aureus* quickly decreased within 3 days period as inhibition diameters decreased from 4.0 cm
347 down to 2.2 cm. On the contrary, the antibacterial activity of PET20-PEM5 samples against *S.*
348 *aureus* only slightly decreased during the 28 days period as inhibition diameters decreased
349 from 5.0 cm down to 3.5 cm. So, diffusion tests realized after ageing samples in batch was
350 maintained at high and almost constant level over at least 28 days against both bacterial
351 strains. The test positive response in the diffusion test indicated that the amount of TCS
352 released from aged samples in the agar gel was always maintained above the minimum
353 inhibitory concentration (MIC). This slow and controlled release can be attributed to the high
354 inclusion complex formation constants reported above between TCS and CD moieties in
355 PCD+ and PCD-.

356 In our previous paper (Junthip et al., 2016), we reported that PET20-PEM5 sample
357 without TCS, tested by the *kill-time* method, displayed bacterial reductions of 7.3 and 4.5
358 log₁₀ against *S. aureus* and *E. coli*. This intrinsic antibacterial activity was found to be
359 dependent of the trimethylammonium content of polyEPG-CD-10 in the self-assembled layer
360 (Junthip et al., 2016). Interestingly, in our former studies dealing with PEM coatings based on
361 PCD- as polyanion, and chitosan as polycations (Aubert-Viard et al., 2019; Martin et al.,
362 2013a; Mogrovejo-Valdivia et al., 2019; Pérez-Anes et al., 2015) control samples not loaded
363 with any antibacterial substances did not display such intrinsic antibacterial activity despite
364 chitosan is often reported as an antibacterial polymer. The presence of quaternary ammonium

365 groups carried by PCD+ versus primary ammonium groups carried by chitosan can explain
366 such result. These previous results combined to our new results showed that these
367 PCD+/PCD- systems presented intrinsic contact killing property and also extrinsic release
368 killing properties once loaded with TCS (up to 28 days).

369

370 **Conclusion**

371 Polyelectrolyte multilayer (PEM) assembly based on water-soluble cationic β -
372 cyclodextrin polymer (polyEPG-CD) and anionic β -cyclodextrin polymer (polyCTR-CD) was
373 built up by the layer-by-layer technique onto non-woven PET textile preliminarily modified
374 by polyCTR-CD through a thermofixation process. TCS loading on the samples coated with 5
375 self-assembled bilayers (PET20-PEM5 samples) reached 4.6 mg/g of textile, against only 1.1
376 mg/g on the sample modified with one thermofixed layer consisting of polyCTR-CD (PET20
377 samples). The PEM system displayed the sustained release of TCS over 14 hours in dynamic
378 conditions. Besides, diffusion tests realized after ageing samples in batch was maintained at
379 high and constant level over at least 28 days. These properties could be explained by the
380 reversible inclusion complex formation between TCS and CD moieties present in both
381 cationic and anionic crosslinked polymers. These results combined to our previous published
382 paper (Junthip et al., 2016) showed that these PCD+/PCD- systems presented intrinsic contact
383 killing property and also extrinsic release killing properties once loaded with TCS.
384 PCD+/PCD- systems offer consequently an excellent potential for the prevention and curing
385 of peri-operative infections on biomedical devices which often display dramatical
386 consequences.

387

388 **Acknowledgements**

389 Thanks to the Royal Thai Government Scholarship allocated upon the Ministry of
390 Science and Technology who supported this work to the first author.

391 Chevreul Institute (FR 2638), Ministère de l'Enseignement Supérieur et de la
392 Recherche, Région Hauts-de-France and FEDER are acknowledged for supporting and
393 funding this work.

394

395 Reference

396 Agarwal, A., Nelson, T.B., Kierski, P.R., Schurr, M.J., Murphy, C.J., Czuprynski, C.J.,
397 McAnulty, J.F., Abbott, N.L., 2012. Polymeric multilayers that localize the release of
398 chlorhexidine from biologic wound dressings. *Biomaterials* 33, 6783–6792.
399 <https://doi.org/10.1016/j.biomaterials.2012.05.068>

400 Assadian, O., Wehse, K., Hübner, N.-O., Koburger, T., Bagel, S., Jethon, F., Kramer, A.,
401 2011. Minimum inhibitory (MIC) and minimum microbicidal concentration (MMC) of
402 polihexanide and triclosan against antibiotic sensitive and resistant *Staphylococcus*
403 *aureus* and *Escherichia coli* strains. *GMS Krankenhaushyg Interdiszip* 6, Doc06.
404 <https://doi.org/10.3205/dgkh000163>

405 Aubert-Viard, F., Mogrovejo-Valdivia, A., Tabary, N., Maton, M., Chai, F., Neut, C., Martel,
406 B., Blanchemain, N., 2019. Evaluation of antibacterial textile covered by layer-by-
407 layer coating and loaded with chlorhexidine for wound dressing application. *Materials*
408 *Science and Engineering: C* 100, 554–563. <https://doi.org/10.1016/j.msec.2019.03.044>

409 Benkirane-Jessel, N., Schwinté, P., Falvey, P., Darcy, R., Häikel, Y., Schaaf, P., Voegel, J.-
410 C., Ogier, J., 2004. Build-up of Polypeptide Multilayer Coatings with Anti-
411 Inflammatory Properties Based on the Embedding of Piroxicam–Cyclodextrin
412 Complexes. *Advanced Functional Materials* 14, 174–182.
413 <https://doi.org/10.1002/adfm.200304413>

414 Boudou, T., Crouzier, T., Ren, K., Blin, G., Picart, C., 2010. Multiple Functionalities of
415 Polyelectrolyte Multilayer Films: New Biomedical Applications. *Advanced Materials*
416 22, 441–467. <https://doi.org/10.1002/adma.200901327>

417 Cai, W., Wu, J., Xi, C., Ashe, A.J., Mark, E.M., 2011. Carboxyl-Ebselen-Based Layer-by-
418 Layer Films as Potential Antithrombotic and Antimicrobial Coatings. *Biomaterials* 32,
419 7774–7784. <https://doi.org/10.1016/j.biomaterials.2011.06.075>

420 Chen, S., Li, L., Zhao, C., Zheng, J., 2010. Surface hydration: Principles and applications
421 toward low-fouling/nonfouling biomaterials. *Polymer* 51, 5283–5293.
422 <https://doi.org/10.1016/j.polymer.2010.08.022>

423 Chen, X., Wu, W., Guo, Z., Xin, J., Li, J., 2011. Controlled insulin release from glucose-
424 sensitive self-assembled multilayer films based on 21-arm star polymer. *Biomaterials*
425 32, 1759–1766. <https://doi.org/10.1016/j.biomaterials.2010.11.002>

426 Cheng, C.-Y., Wang, Y.-C., Chen, H.-C., Ding, W.-H., 2011. Simplified Derivatization
427 Method for Triclosan Determination in Personal Care Products by Gas
428 Chromatography-Mass Spectrometry. *Journal of the Chinese Chemical Society* 58,
429 49–52. <https://doi.org/10.1002/jccs.201190057>

- 430 Chuang, H.F., Smith, R.C., Hammond, P.T., 2008. Polyelectrolyte Multilayers for Tunable
431 Release of Antibiotics. *Biomacromolecules* 9, 1660–1668.
432 <https://doi.org/10.1021/bm800185h>
- 433 Dai, J., Bruening, M.L., 2002. Catalytic Nanoparticles Formed by Reduction of Metal Ions in
434 Multilayered Polyelectrolyte Films. *Nano Lett.* 2, 497–501.
435 <https://doi.org/10.1021/nl0255471>
- 436 Decher, G., Hong, J.D., Schmitt, J., 1992. Buildup of ultrathin multilayer films by a self-
437 assembly process: III. Consecutively alternating adsorption of anionic and cationic
438 polyelectrolytes on charged surfaces. *Thin Solid Films* 210–211, 831–835.
439 [https://doi.org/10.1016/0040-6090\(92\)90417-A](https://doi.org/10.1016/0040-6090(92)90417-A)
- 440 Duan, M.S., Zhao, N., Ossurardóttir, I.B., Thorsteinsson, T., Loftsson, T., 2005. Cyclodextrin
441 solubilization of the antibacterial agents triclosan and triclocarban: formation of
442 aggregates and higher-order complexes. *Int J Pharm* 297, 213–222.
443 <https://doi.org/10.1016/j.ijpharm.2005.04.007>
- 444 Ducoroy, L., Bacquet, M., Martel, B., Morcellet, M., 2008. Removal of heavy metals from
445 aqueous media by cation exchange nonwoven PET coated with β -cyclodextrin-
446 polycarboxylic moieties. *Reactive and Functional Polymers* 68, 594–600.
447 <https://doi.org/10.1016/j.reactfunctpolym.2007.10.033>
- 448 Fagui, A.E., Wintgens, V., Gaillet, C., Dubot, P., Amiel, C., 2014. Layer-by-Layer Coated
449 PLA Nanoparticles with Oppositely Charged β -Cyclodextrin Polymer for Controlled
450 Delivery of Lipophilic Molecules. *Macromolecular Chemistry and Physics* 215, 555–
451 565. <https://doi.org/10.1002/macp.201300693>
- 452 Genzer, J., Efimenko, K., 2006. Recent developments in superhydrophobic surfaces and their
453 relevance to marine fouling: a review. *Biofouling* 22, 339–360.
454 <https://doi.org/10.1080/08927010600980223>
- 455 Graisuwan, W., Wiarachai, O., Ananthanawat, C., Puthong, S., Soogarun, S.,
456 Kiatkamjornwong, S., Hoven, V.P., 2012. Multilayer film assembled from charged
457 derivatives of chitosan: physical characteristics and biological responses. *J Colloid*
458 *Interface Sci* 376, 177–188. <https://doi.org/10.1016/j.jcis.2012.02.039>
- 459 Hammond, P.T., 2012. Building biomedical materials layer-by-layer. *Materials Today* 15,
460 196–206. [https://doi.org/10.1016/S1369-7021\(12\)70090-1](https://doi.org/10.1016/S1369-7021(12)70090-1)
- 461 Higuchi, T., Connors, K., 1965. Phase Solubility Techniques. *Advanced Analytical Chemistry*
462 *of Instrumentation* 4, 117–212.
- 463 Jones, R.D., Jampani, H.B., Newman, J.L., Lee, A.S., 2000. Triclosan: a review of
464 effectiveness and safety in health care settings. *Am J Infect Control* 28, 184–196.
- 465 Jug, M., Kosalec, I., Maestrelli, F., Mura, P., 2011. Analysis of triclosan inclusion complexes
466 with β -cyclodextrin and its water-soluble polymeric derivative. *J Pharm Biomed Anal*
467 54, 1030–1039. <https://doi.org/10.1016/j.jpba.2010.12.009>
- 468 Junthip, J., Tabary, N., Chai, F., Leclercq, L., Maton, M., Cazaux, F., Neut, C., Paccou, L.,
469 Guinet, Y., Staelens, J.-N., Bria, M., Landy, D., Hédoux, A., Blanchemain, N., Martel,
470 B., 2016. Layer-by-layer coating of textile with two oppositely charged cyclodextrin
471 polyelectrolytes for extended drug delivery. *J Biomed Mater Res A* 104, 1408–1424.
472 <https://doi.org/10.1002/jbm.a.35674>
- 473 Junthip, J., Tabary, N., Leclercq, L., Martel, B., 2015. Cationic β -cyclodextrin polymer
474 applied to a dual cyclodextrin polyelectrolyte multilayer system. *Carbohydr Polym*
475 126, 156–167. <https://doi.org/10.1016/j.carbpol.2015.02.064>
- 476 Leguen, E., Chassepot, A., Decher, G., Schaaf, P., Voegel, J.-C., Jessel, N., 2007. Bioactive
477 coatings based on polyelectrolyte multilayer architectures functionalized by embedded
478 proteins, peptides or drugs. *Biomol. Eng.* 24, 33–41.
479 <https://doi.org/10.1016/j.bioeng.2006.05.023>

480 Lichter, J.A., Rubner, M.F., 2009. Polyelectrolyte Multilayers with Intrinsic Antimicrobial
481 Functionality: The Importance of Mobile Polycations. *Langmuir* 25, 7686–7694.
482 <https://doi.org/10.1021/la900349c>

483 Lichter, J.A., Thompson, M.T., Delgadillo, M., Nishikawa, T., Rubner, M.F., Van Vliet, K.J.,
484 2008. Substrata mechanical stiffness can regulate adhesion of viable bacteria.
485 *Biomacromolecules* 9, 1571–1578. <https://doi.org/10.1021/bm701430y>

486 Lichter, J.A., Van Vliet, K.J., Rubner, M.F., 2009. Design of Antibacterial Surfaces and
487 Interfaces: Polyelectrolyte Multilayers as a Multifunctional Platform. *Macromolecules*
488 42, 8573–8586. <https://doi.org/10.1021/ma901356s>

489 Loftsson, T., Leeves, N., Bjornsdottir, B., Duffy, L., Masson, M., 1999. Effect of
490 cyclodextrins and polymers on triclosan availability and substantivity in toothpastes in
491 vivo. *J Pharm Sci* 88, 1254–1258. <https://doi.org/10.1021/js9902466>

492 Lu, J., Hill, M.A., Hood, M., Greeson, D.F., Horton, J.R., Orndorff, P.E., Herndon, A.S.,
493 Tonelli, A.E., 2001. Formation of antibiotic, biodegradable polymers by processing
494 with Irgasan DP300R (triclosan) and its inclusion compound with β -cyclodextrin.
495 *Journal of Applied Polymer Science* 82, 300–309. <https://doi.org/10.1002/app.1852>

496 Martel, B., Ruffin, D., Weltrowski, M., Lekchiri, Y., Morcellet, M., 2005. Water-soluble
497 polymers and gels from the polycondensation between cyclodextrins and
498 poly(carboxylic acid)s: A study of the preparation parameters. *Journal of Applied*
499 *Polymer Science* 97, 433–442. <https://doi.org/10.1002/app.21391>

500 Martin, A., Tabary, N., Chai, F., Leclercq, L., Junthip, J., Aubert-Viard, F., Neut, C.,
501 Weltrowski, M., Blanchemain, N., Martel, B., 2013a. Build-up of an antimicrobial
502 multilayer coating on a textile support based on a methylene blue-poly(cyclodextrin)
503 complex. *Biomed Mater* 8, 065006. <https://doi.org/10.1088/1748-6041/8/6/065006>

504 Martin, A., Tabary, N., Leclercq, L., Junthip, J., Degoutin, S., Aubert-Viard, F., Cazaux, F.,
505 Lyskawa, J., Janus, L., Bria, M., Martel, B., 2013b. Multilayered textile coating based
506 on a β -cyclodextrin polyelectrolyte for the controlled release of drugs. *Carbohydr*
507 *Polym* 93, 718–730. <https://doi.org/10.1016/j.carbpol.2012.12.055>

508 Mogrovejo-Valdivia, A., Rahmouni, O., Tabary, N., Maton, M., Neut, C., Martel, B.,
509 Blanchemain, N., 2019. In vitro evaluation of drug release and antibacterial activity of
510 a silver-loaded wound dressing coated with a multilayer system. *International Journal*
511 *of Pharmaceutics* 556, 301–310. <https://doi.org/10.1016/j.ijpharm.2018.12.018>

512 Nguyen, P.M., Zacharia, N.S., Verploegen, E., Hammond, P.T., 2007. Extended Release
513 Antibacterial Layer-by-Layer Films Incorporating Linear-Dendritic Block Copolymer
514 Micelles. *Chem. Mater.* 19, 5524–5530. <https://doi.org/10.1021/cm070981f>

515 Pérez-Anes, A., Gargouri, M., Laure, W., Van Den Berghe, H., Courcot, E., Sobocinski, J.,
516 Tabary, N., Chai, F., Blach, J.-F., Addad, A., Woisel, P., Douroumis, D., Martel, B.,
517 Blanchemain, N., Lyskawa, J., 2015. Bioinspired Titanium Drug Eluting Platforms
518 Based on a Poly- β -cyclodextrin–Chitosan Layer-by-Layer Self-Assembly Targeting
519 Infections. *ACS Appl. Mater. Interfaces* 7, 12882–12893.
520 <https://doi.org/10.1021/acsami.5b02402>

521 Phelps, J.A., Morisse, S., Hindié, M., Degat, M.-C., Pauthe, E., Van Tassel, P.R., 2011.
522 Nanofilm Biomaterials: Localized Cross-Linking To Optimize Mechanical Rigidity
523 and Bioactivity. *Langmuir* 27, 1123–1130. <https://doi.org/10.1021/la104156c>

524 Qian, L., Guan, Y., Xiao, H., 2008. Preparation and characterization of inclusion complexes
525 of a cationic β -cyclodextrin polymer with butylparaben or triclosan. *International*
526 *Journal of Pharmaceutics* 357, 244–251. <https://doi.org/10.1016/j.ijpharm.2008.01.018>

527 Séon, L., Lavalle, P., Schaaf, P., Boulmedais, F., 2015. Polyelectrolyte Multilayers: A
528 Versatile Tool for Preparing Antimicrobial Coatings. *Langmuir* 31, 12856–12872.
529 <https://doi.org/10.1021/acs.langmuir.5b02768>

- 530 Shukla, A., Fleming, K.E., Chuang, H.F., Chau, T.M., Loose, C.R., Stephanopoulos, G.N.,
 531 Hammond, P.T., 2010. Controlling the release of peptide antimicrobial agents from
 532 surfaces. *Biomaterials* 31, 2348–2357.
 533 <https://doi.org/10.1016/j.biomaterials.2009.11.082>
- 534 Smith, R.C., Riollano, M., Leung, A., Hammond, P.T., 2009. Layer-by-Layer Platform
 535 Technology for Small-Molecule Delivery. *Angewandte Chemie International Edition*
 536 48, 8974–8977. <https://doi.org/10.1002/anie.200902782>
- 537 Suller, M.T.E., Russell, A.D., 2000. Triclosan and antibiotic resistance in *Staphylococcus*
 538 *aureus*. *J Antimicrob Chemother* 46, 11–18. <https://doi.org/10.1093/jac/46.1.11>
- 539 Teo, B.M., Lyng, M.E., Hosta-Rigau, L., Städler, B., 2015. Subcompartmentalized Surface-
 540 Adhering Polymer Thin Films Toward Drug Delivery Applications, in: *Layer-by-*
 541 *Layer Films for Biomedical Applications*. John Wiley & Sons, Ltd, pp. 207–232.
 542 <https://doi.org/10.1002/9783527675869.ch10>
- 543 Wang, X., Wang, Yan, Bi, S., Wang, Yongguo, Chen, X., Qiu, L., Sun, J., 2014. Optically
 544 Transparent Antibacterial Films Capable of Healing Multiple Scratches. *Advanced*
 545 *Functional Materials* 24, 403–411. <https://doi.org/10.1002/adfm.201302109>
- 546 Wang, Y., Hong, Q., Chen, Y., Lian, X., Xiong, Y., 2012. Surface properties of polyurethanes
 547 modified by bioactive polysaccharide-based polyelectrolyte multilayers. *Colloids Surf*
 548 *B Biointerfaces* 100, 77–83. <https://doi.org/10.1016/j.colsurfb.2012.05.030>
- 549 Wong, S.Y., Moskowitz, J.S., Veselinovic, J., Rosario, R.A., Timachova, K., Blaisse, M.R.,
 550 Fuller, R.C., Klibanov, A.M., Hammond, P.T., 2010. Dual functional polyelectrolyte
 551 multilayer coatings for implants: permanent microbicidal base with controlled release
 552 of therapeutic agents. *J. Am. Chem. Soc.* 132, 17840–17848.
 553 <https://doi.org/10.1021/ja106288c>
- 554 Yazdankhah, S.P., Scheie, A.A., Høiby, E.A., Lunestad, B.-T., Heir, E., Fotland, T.Ø.,
 555 Naterstad, K., Kruse, H., 2006. Triclosan and antimicrobial resistance in bacteria: an
 556 overview. *Microb. Drug Resist.* 12, 83–90. <https://doi.org/10.1089/mdr.2006.12.83>
- 557 Zhu, X., Jańczewski, D., Guo, S., Lee, S.S.C., Parra Velandia, F.J., Teo, S.L.-M., He, T.,
 558 Puniredd, S.R., Vancso, G.J., 2015. Polyion Multilayers with Precise Surface Charge
 559 Control for Antifouling. *ACS Appl. Mater. Interfaces* 7, 852–861.
 560 <https://doi.org/10.1021/am507371a>
- 561 Zhu, X., Loh, X.J., 2015. Layer-by-layer assemblies for antibacterial applications. *Biomater.*
 562 *Sci.* 3, 1505–1518. <https://doi.org/10.1039/C5BM00307E>

564 **Figure captions**

565

566 **Figure 1.** Schematic representation of cationic and anionic polyelectrolytes based on cyclodextrins (PCD- and
 567 PCD+) and of a nonwoven PET coated with an LbL film made of PCD+/PCD- bilayers, stabilized by a thermal
 568 crosslinking reaction at 140°C and loaded with Triclosan

569

570 **Figure 2.** SEM pictures of (a) and (d) virgin PET, (b) and (e) 20%wt thermofixed layer, (c) and (f) multilayers
 571 (10 layers). Magnification x 150 and x800 resolution; full scale 50 and 300 µm.

572

573 **Figure 3.** NMR study of TCS/polyEPG-CD-10 and TCS/polyCTR-CD complexation in D₂O.
574 ¹H NMR of the TCS/polyCTR-CD complex (a), the TCS/polyEPG-CD-10 complex (b) and the magnification at
575 6-8 ppm of TCS (c1), TCS/polyCTR-CD complex (c2) and TCS/polyEPG-CD-10 complex (c3).

576

577 **Figure 4.** Phase solubility diagrams of TCS with (a) βCD and (b) polyEPG-CD-10 and (c) polyCTR-CD, in
578 phosphate buffer (50 mM, pH 6.5) at 25°C.

579

580 **Figure 5.** Release kinetics study of TCS (dynamic mode at 50mL/min, in PBS at 37°C) from thermofixed
581 (PET20) and 5 bilayers (PET20-PEM5) textile samples with (a) TCS released capacity in mg/g of sample, (b)
582 TCS release capacity in %

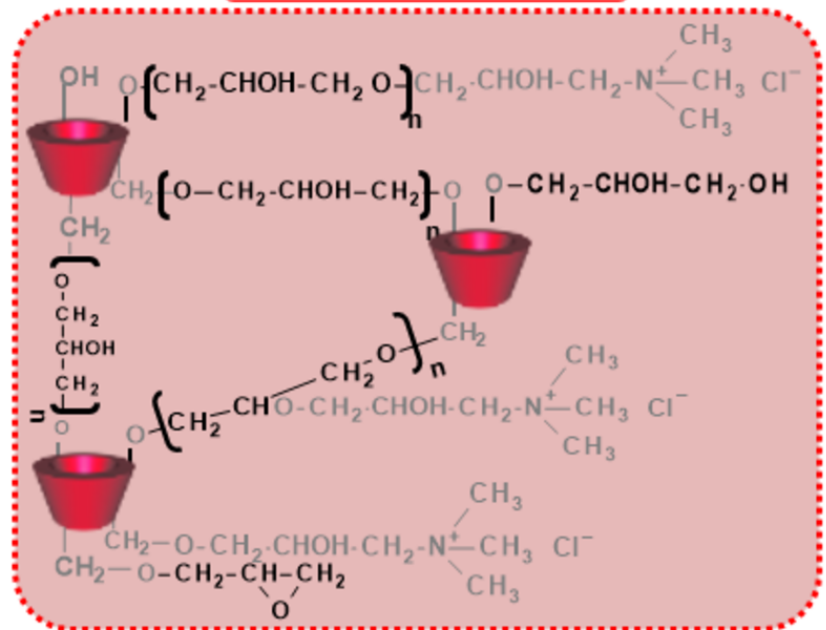
583

584 **Figure 6.** (a) Representative images of Kirby-Bauer test on TCS impregnated PET20 and PET20-PEM5
585 samples against *S. aureus* and *E. coli* with inhibition zone after 24 hours of TCS release in PBS at 37°C.
586 Inhibition zone diameters around PET20 and PET20-PEM5 samples loaded with triclosan (TCS) against (b) *S.*
587 *aureus* and (c) *E. coli* in function of contact time in PBS at 37°C after 24 hours incubation at 37°C over 28 days.

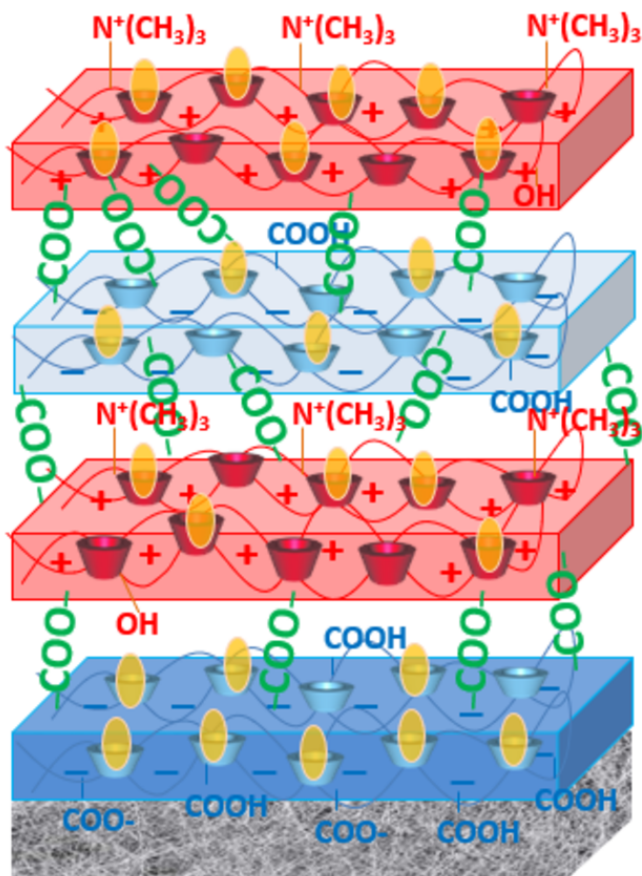
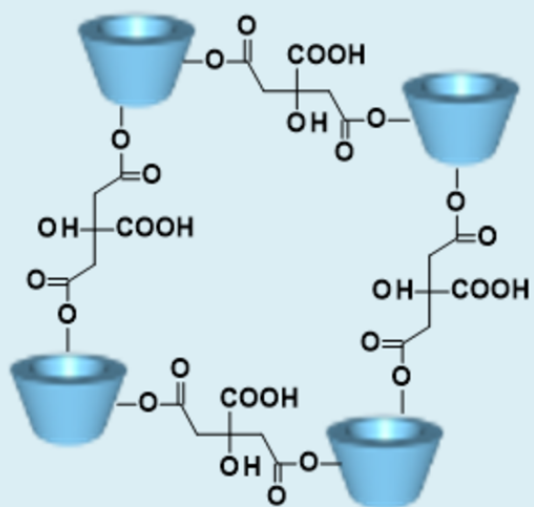
588

589 **Figure S1.** 2D-NOESY NMR spectra of TCS/polyCTR-CD (a) and TCS/polyEPG-CD-10 (b) complexes.

poly-EPG-CD-10 = PCD+



polyCTR-CD = PCD-



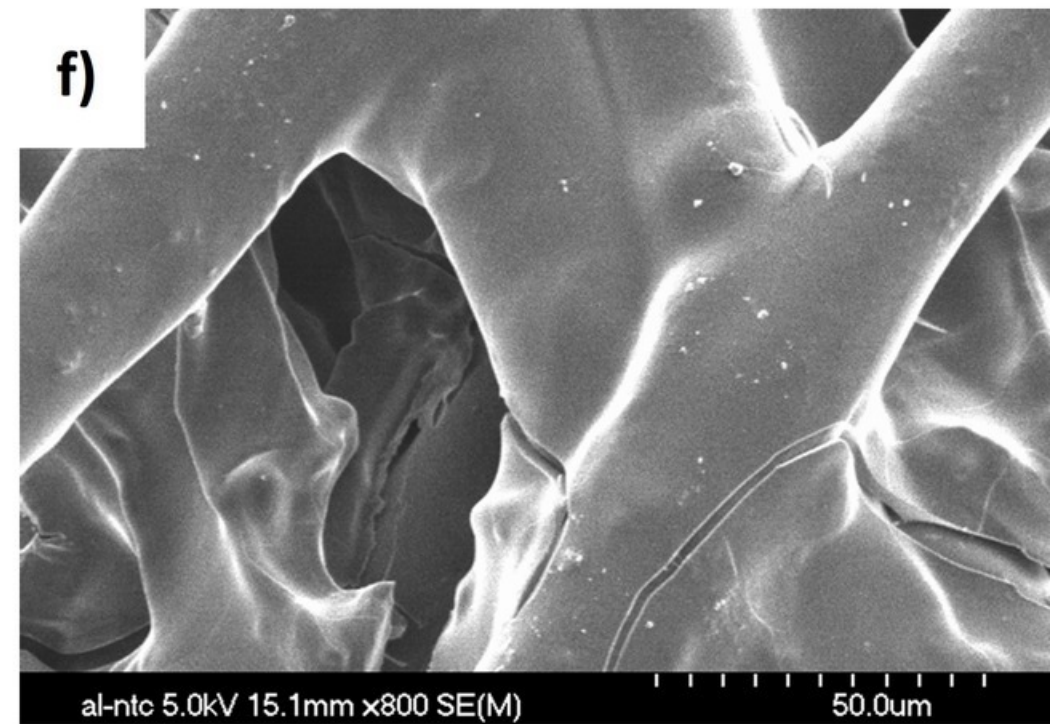
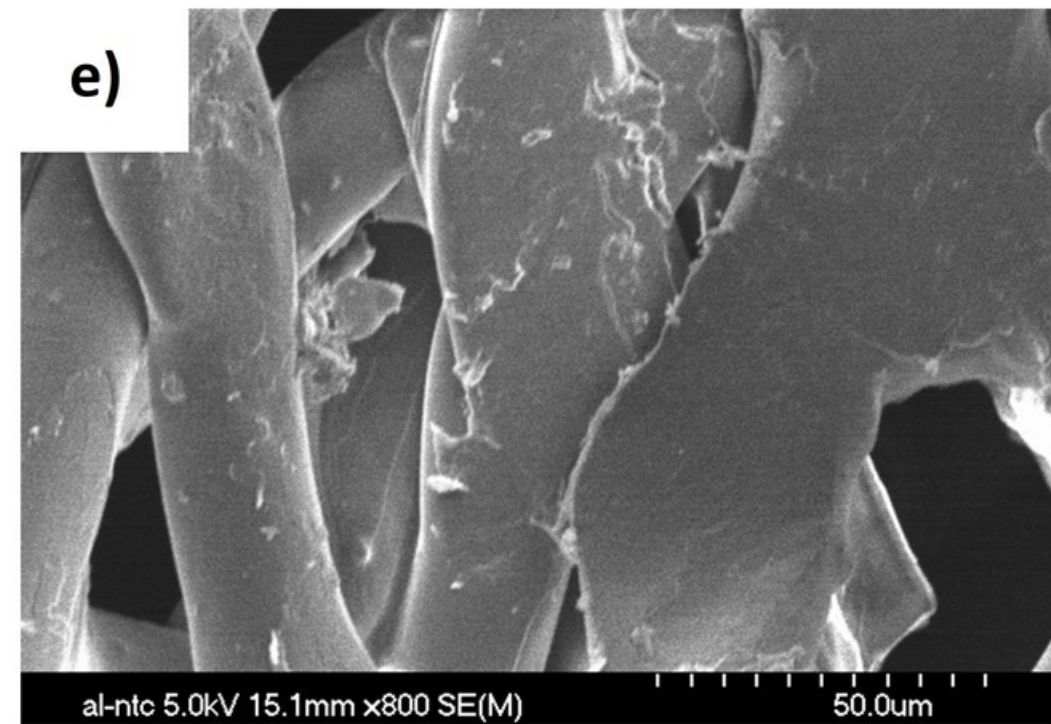
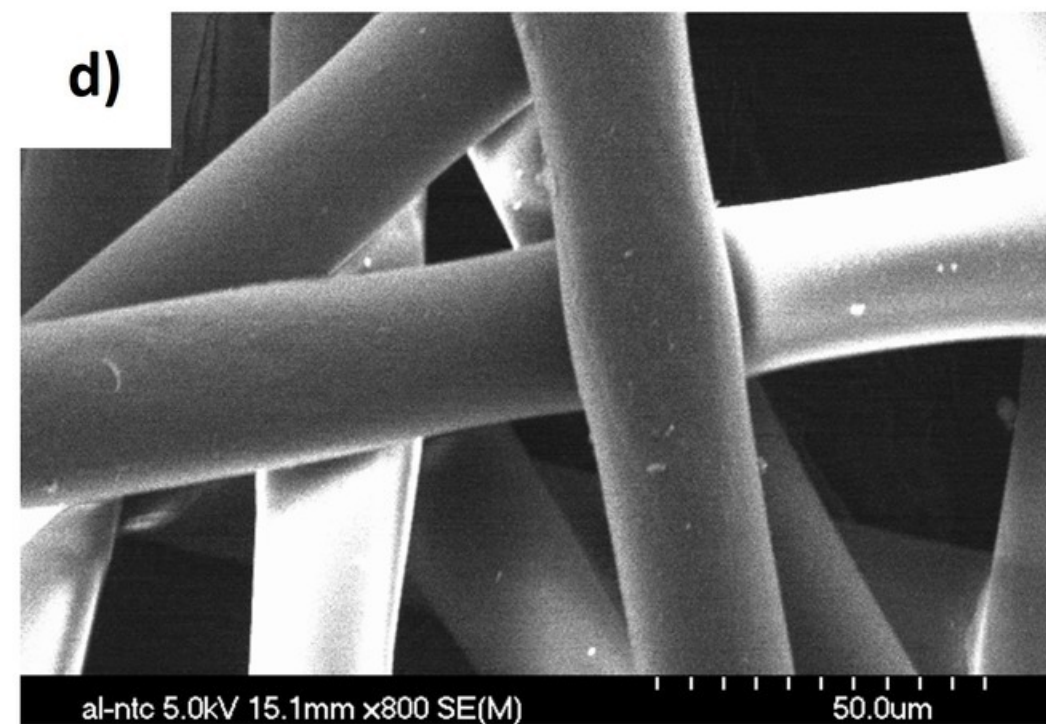
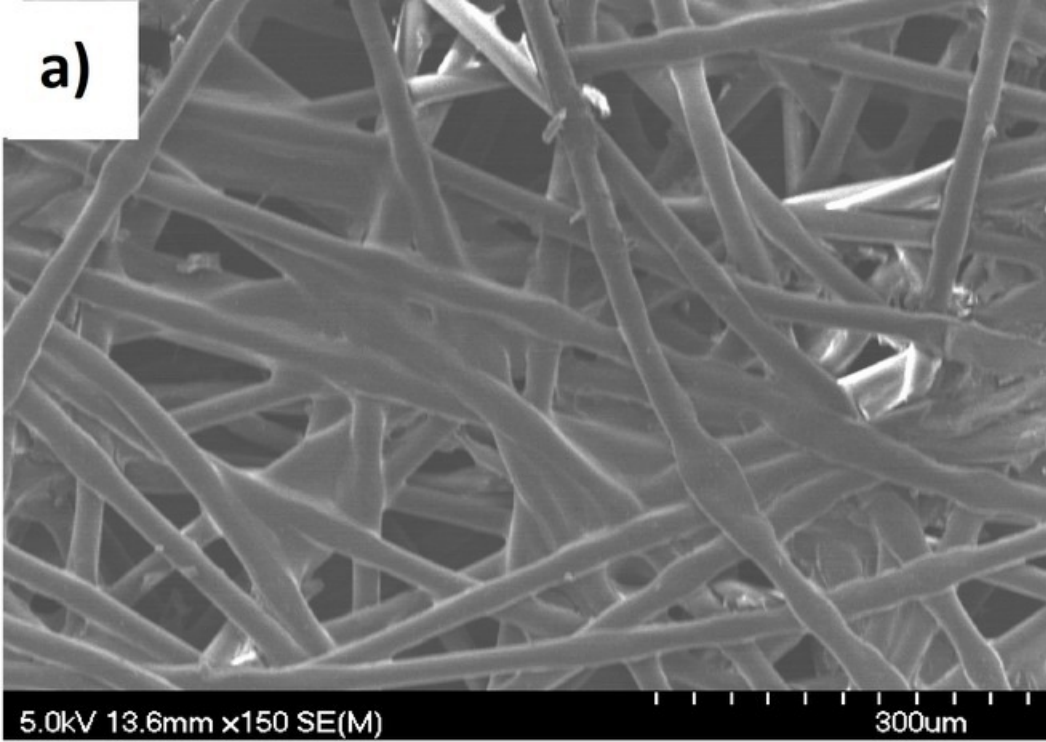
● Triclosan

Self assembled polyCTR-CD

Self assembled poly-EPG-CD-10

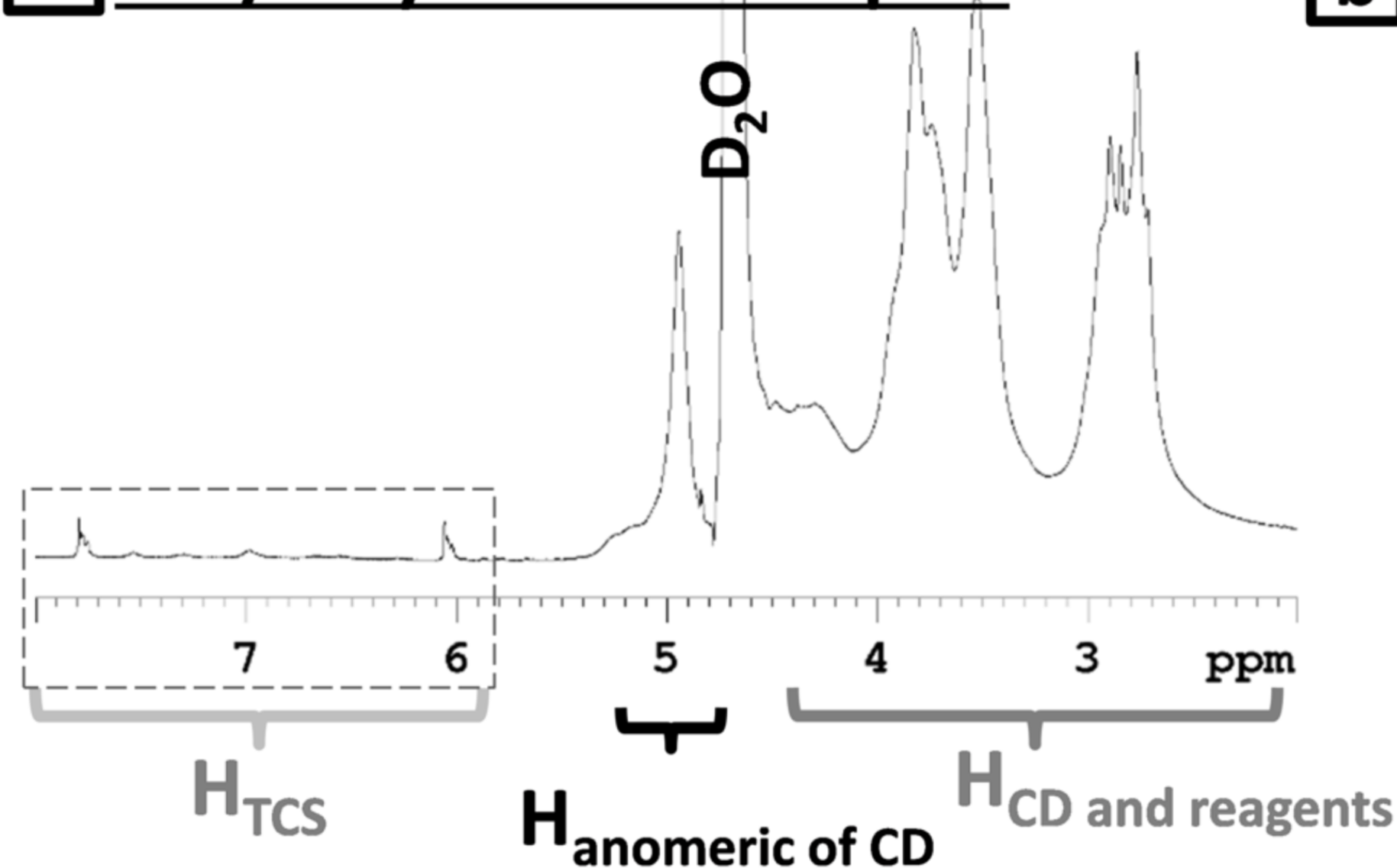
Ester link formed by post-treatment at 140°C

Nonwoven with thermofixed polyCTR-CD layer

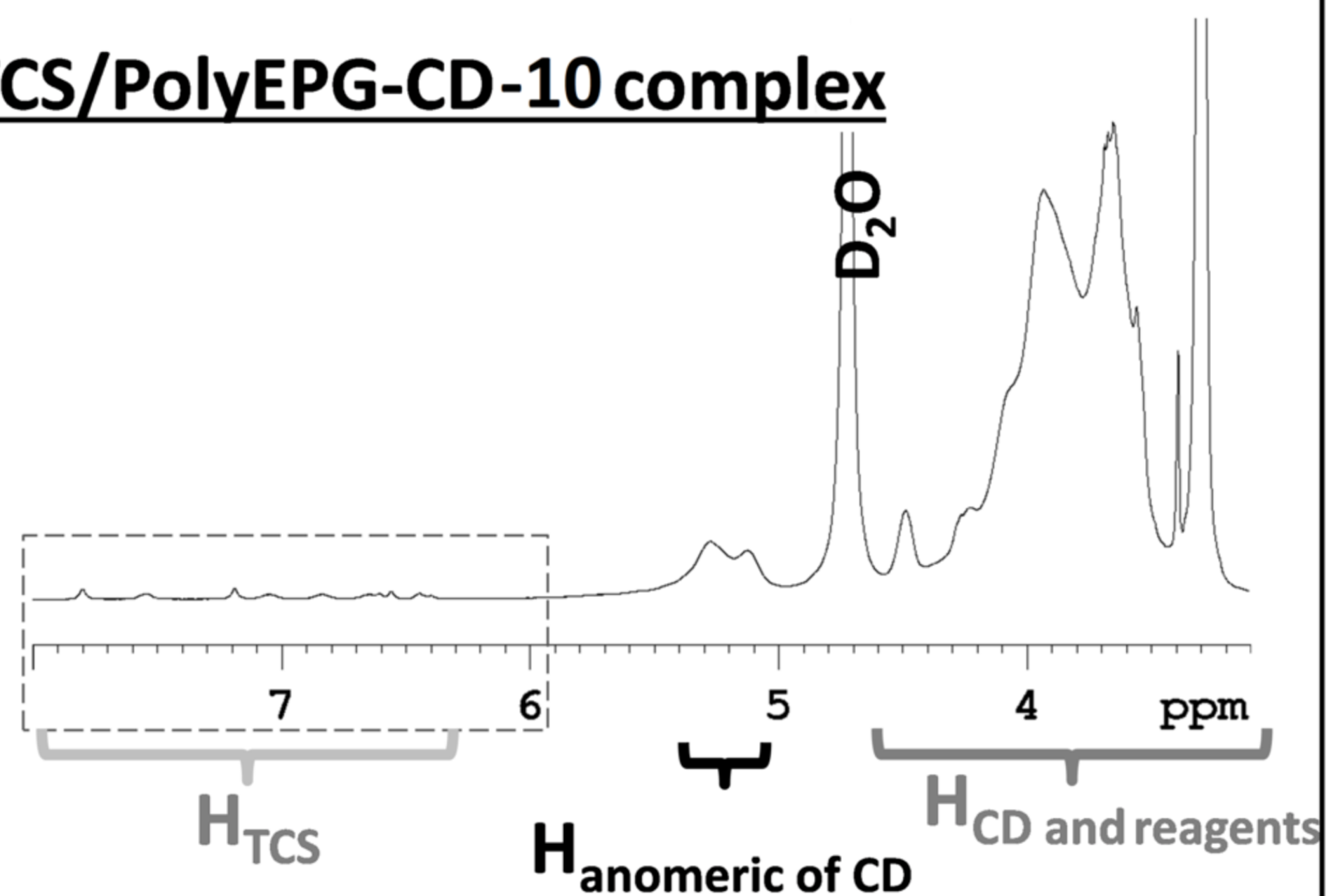


1D ^1H NMR (D_2O)

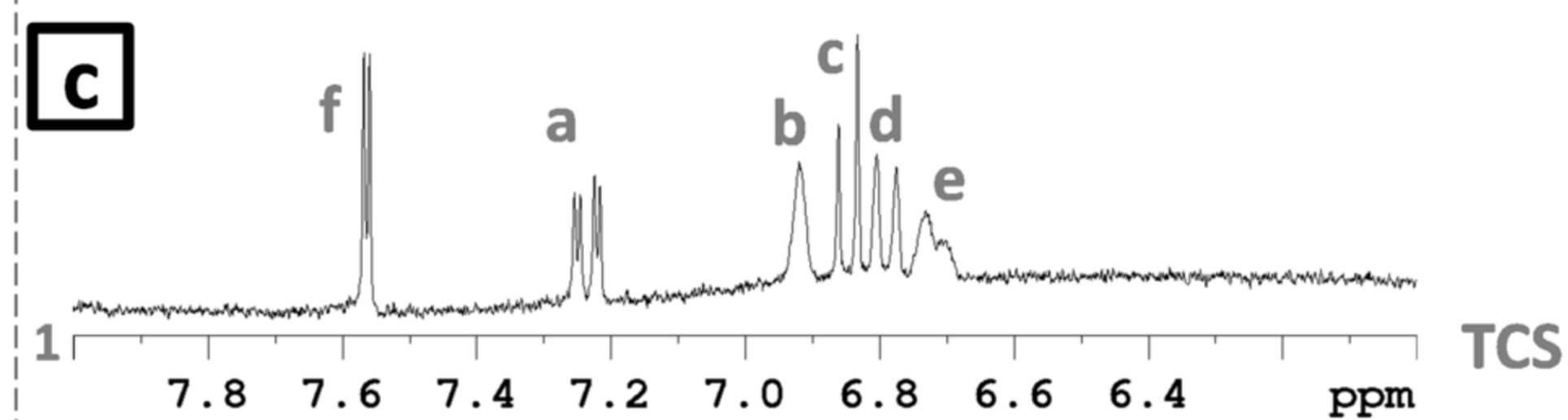
a TCS/PolyCTR-CD complex



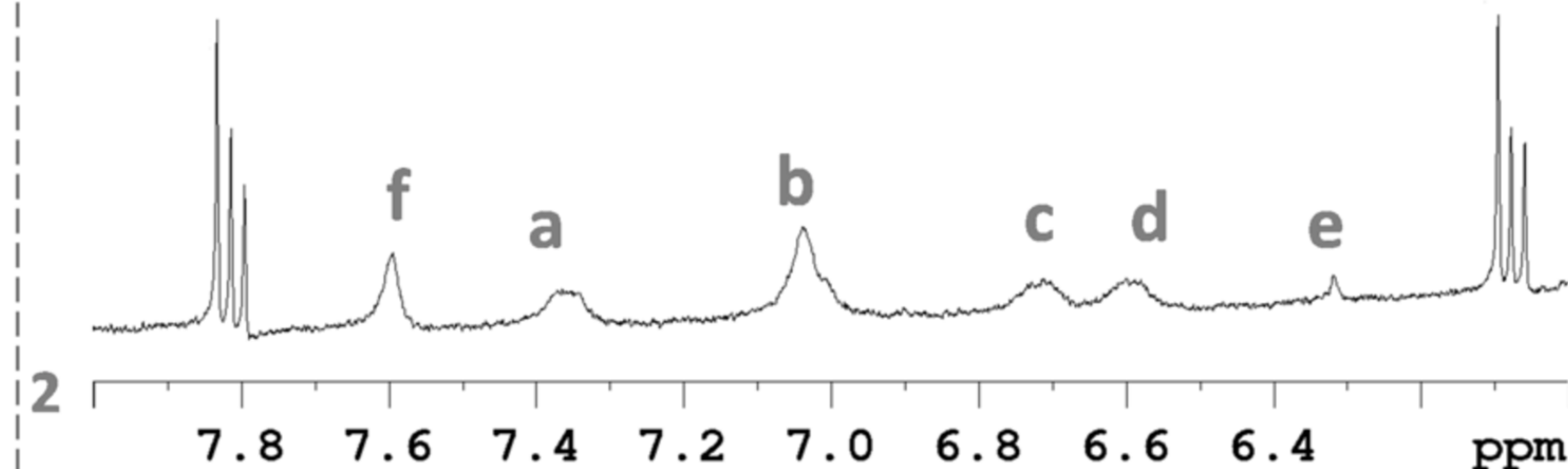
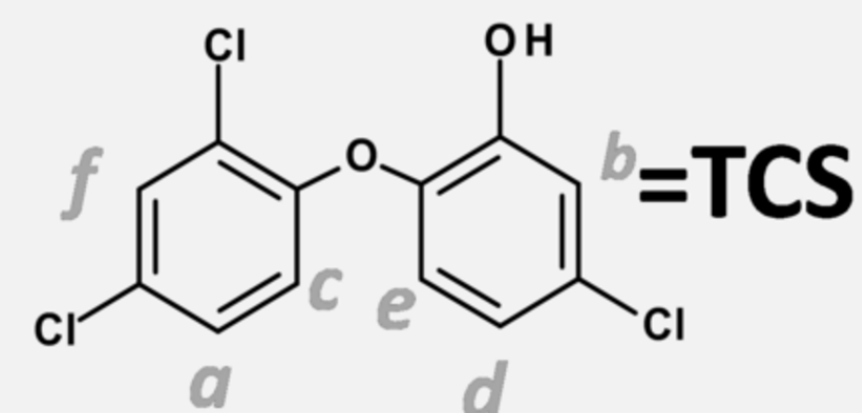
b TCS/PolyEPG-CD-10 complex



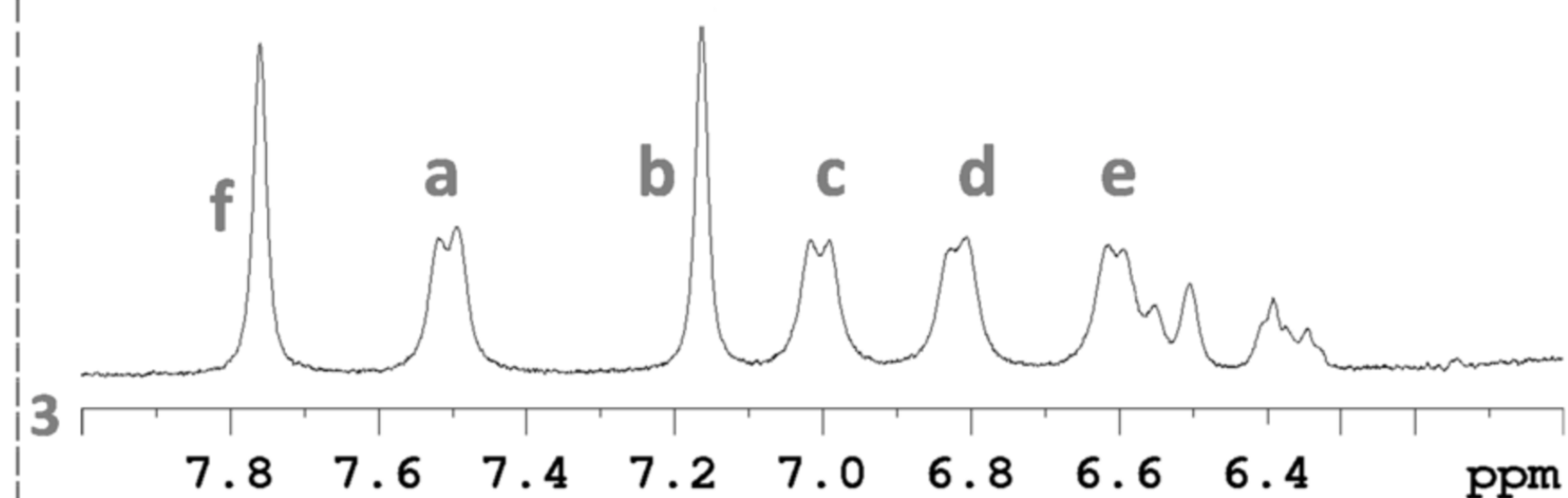
c



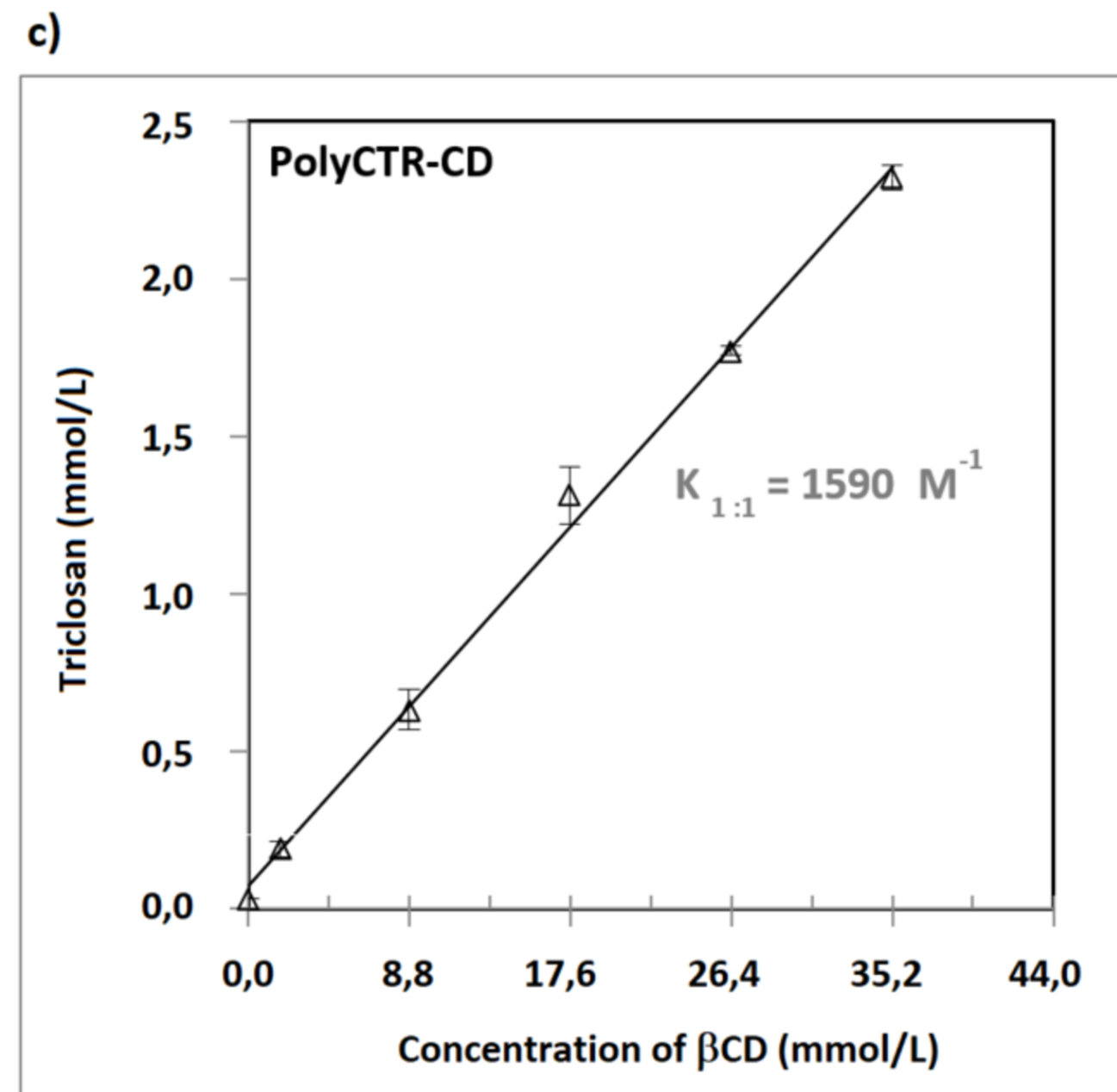
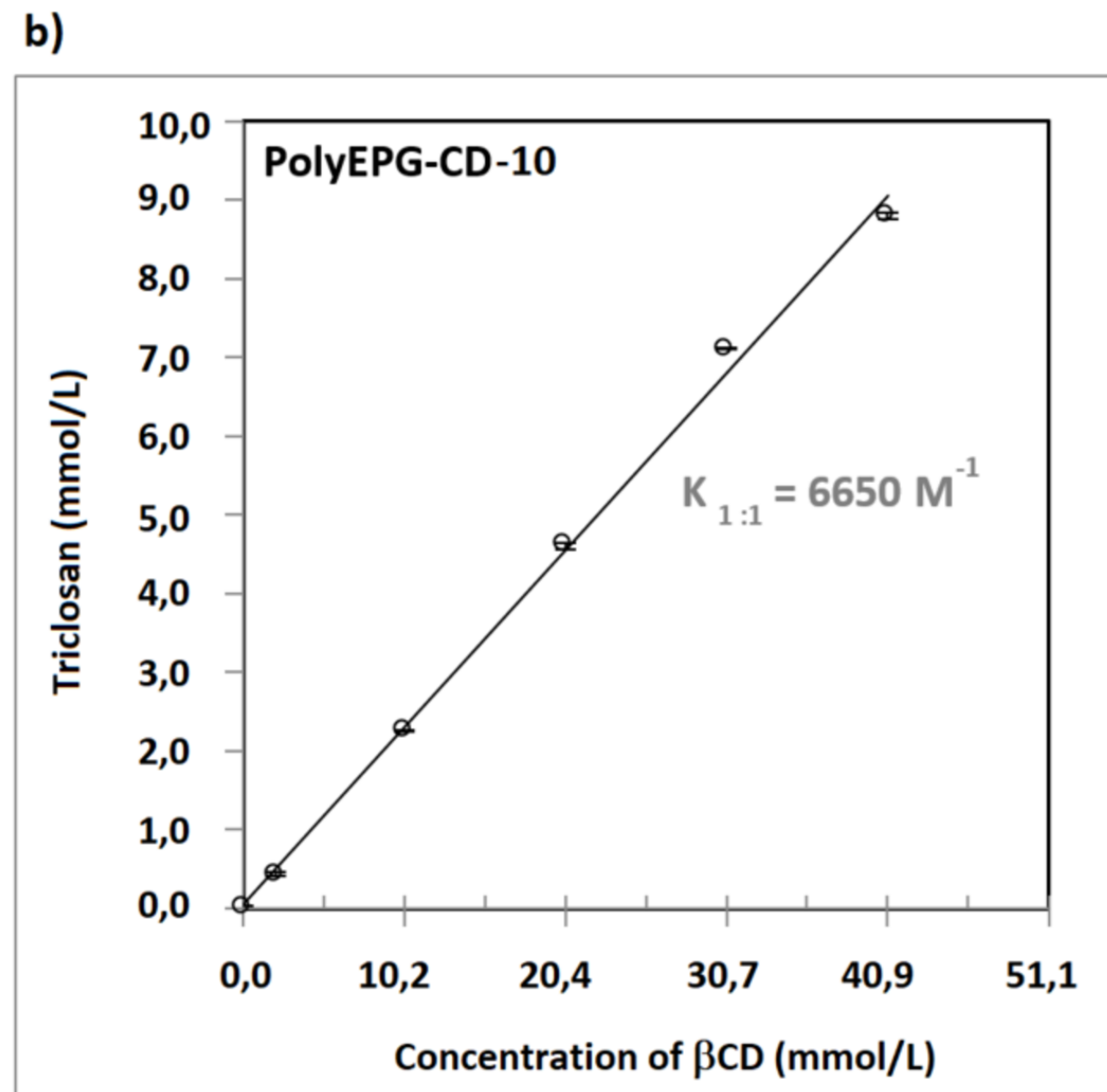
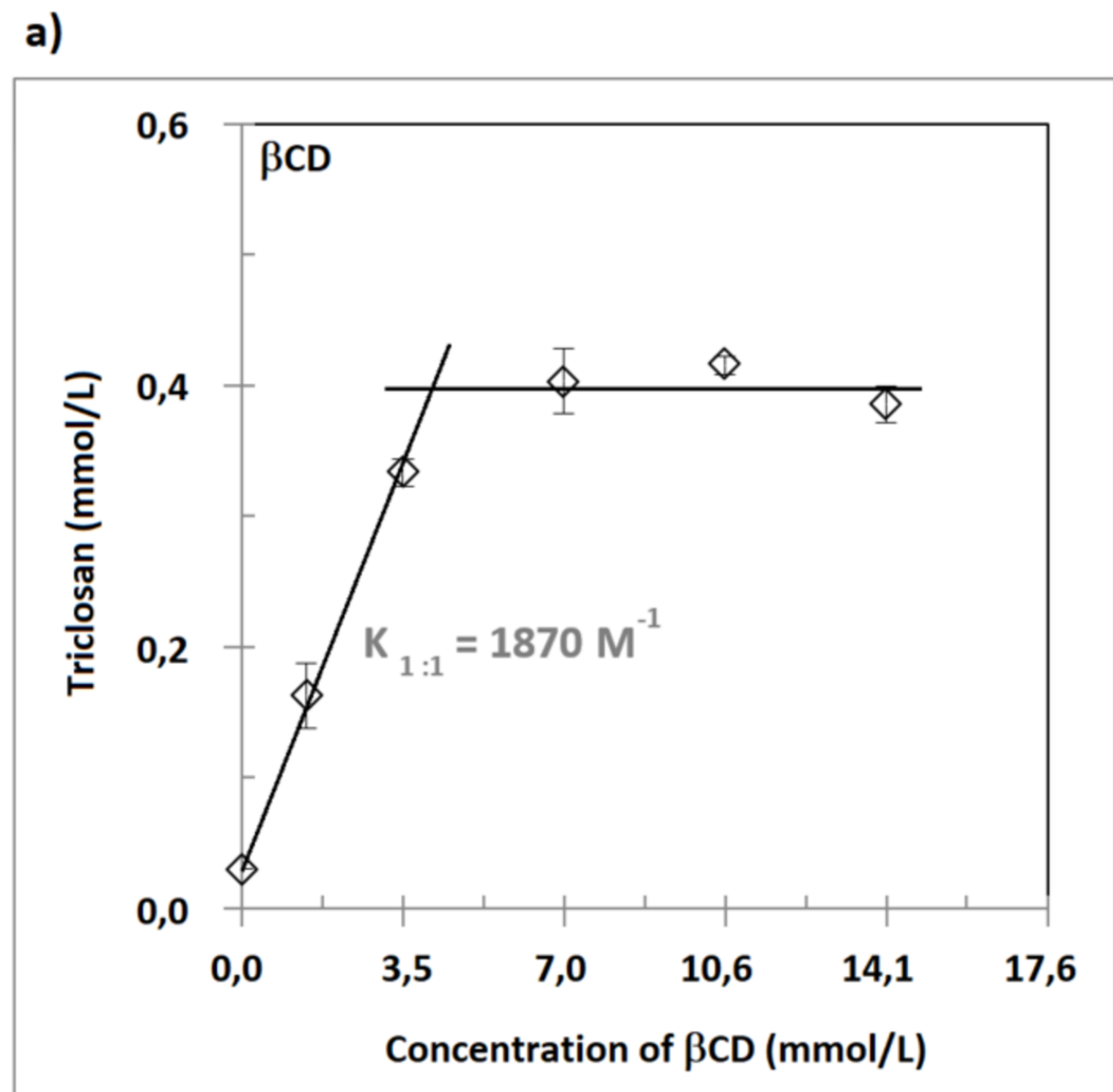
Zoom at 6-8 ppm

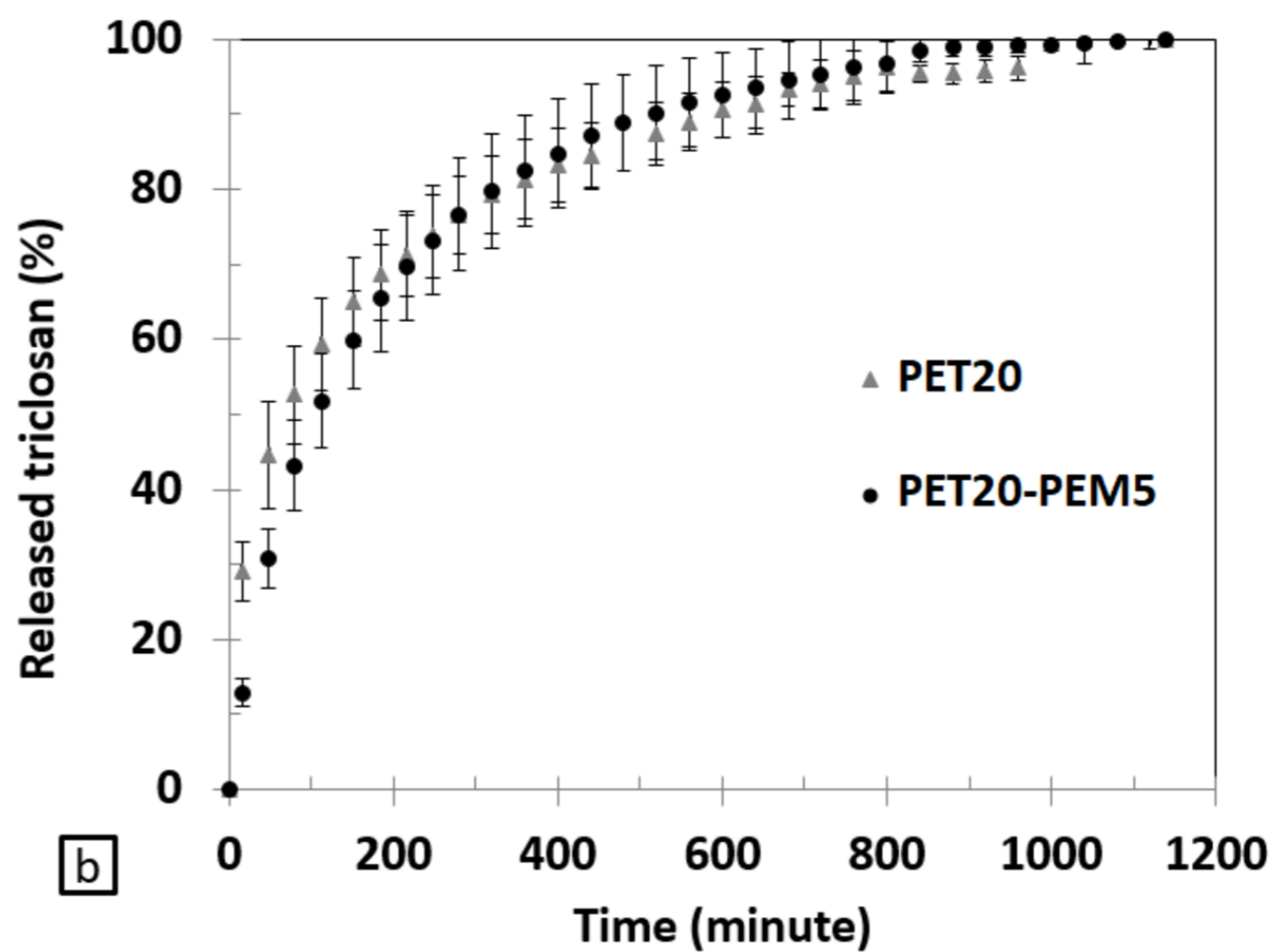
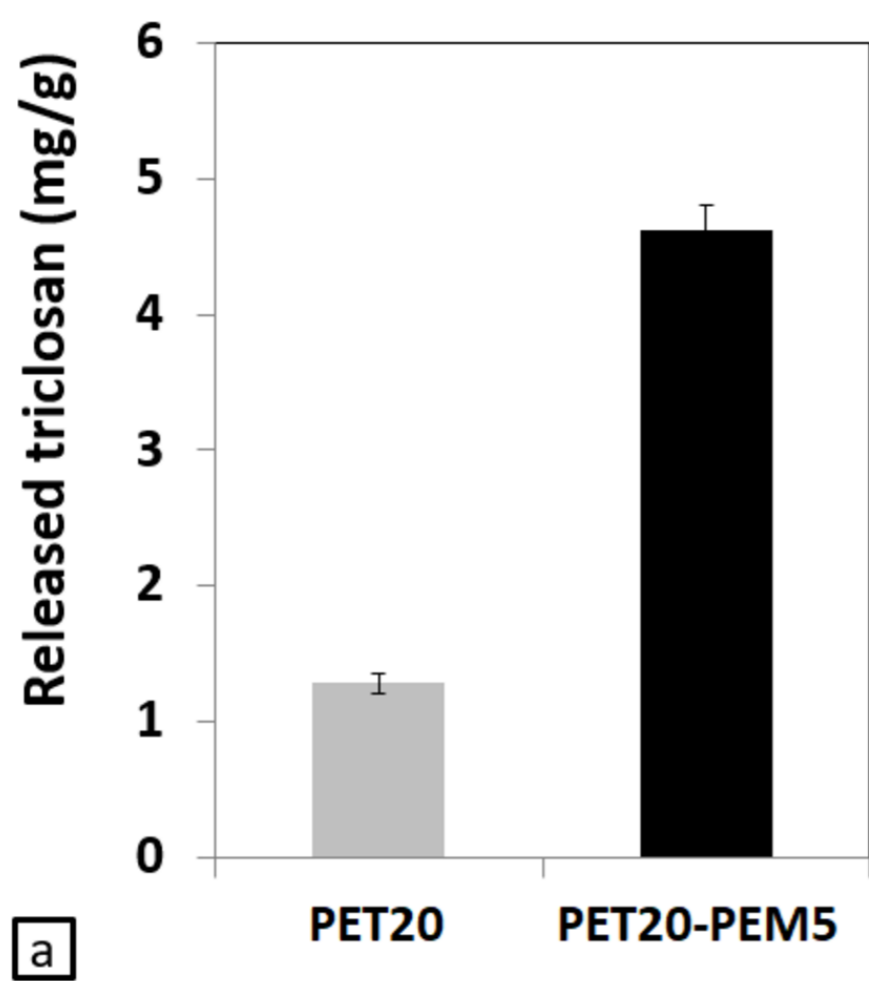


TCS/PolyCTR-CD complex

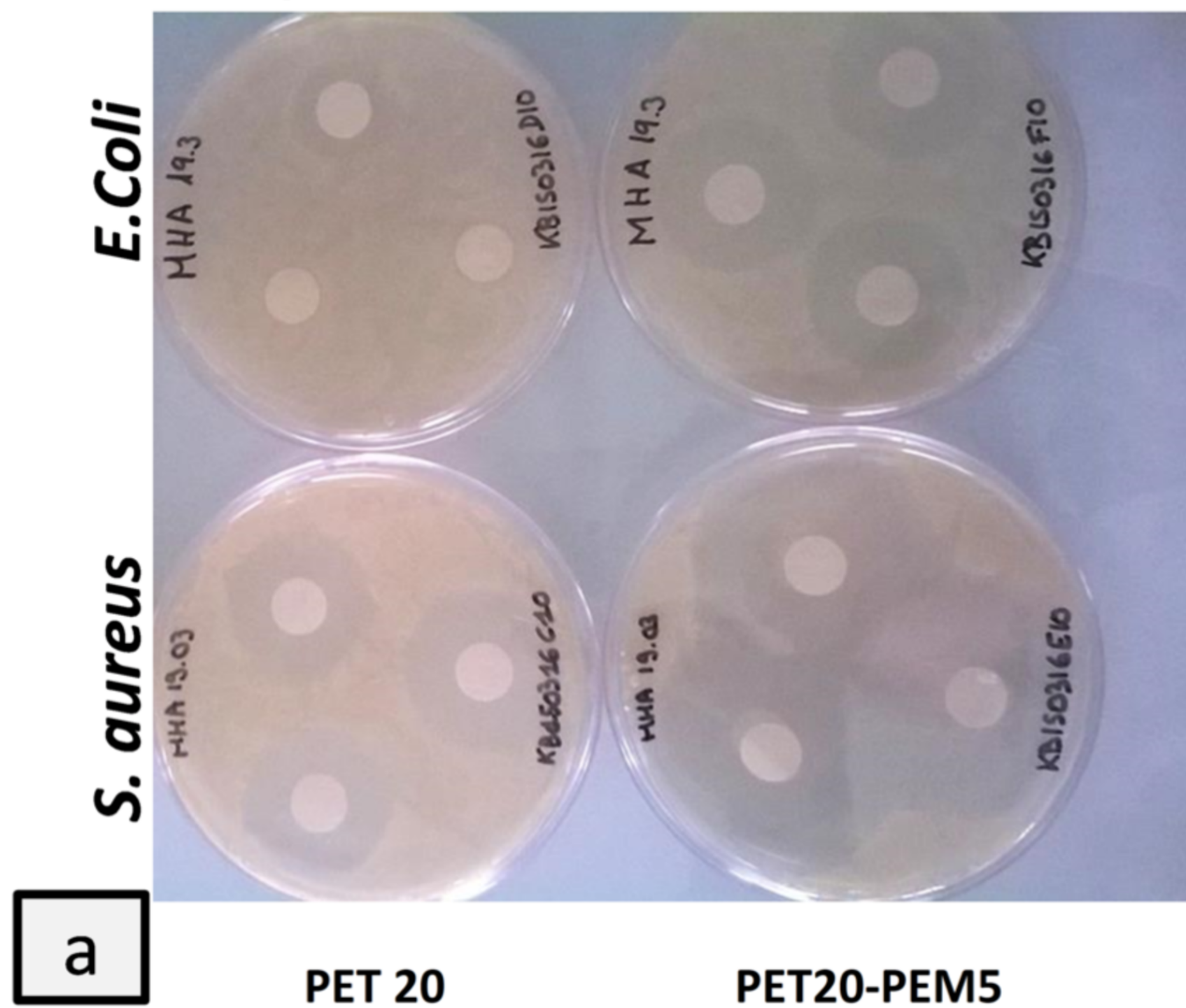


TCS/PolyEPG-CD-10 complex





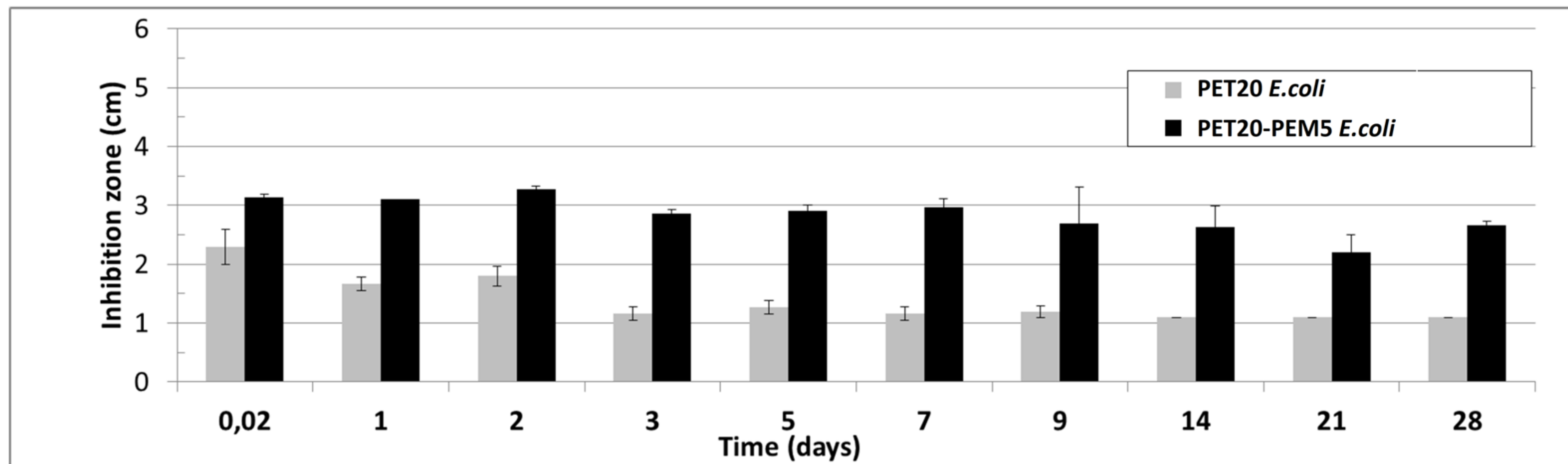
Samples after 24 hours of TCS release



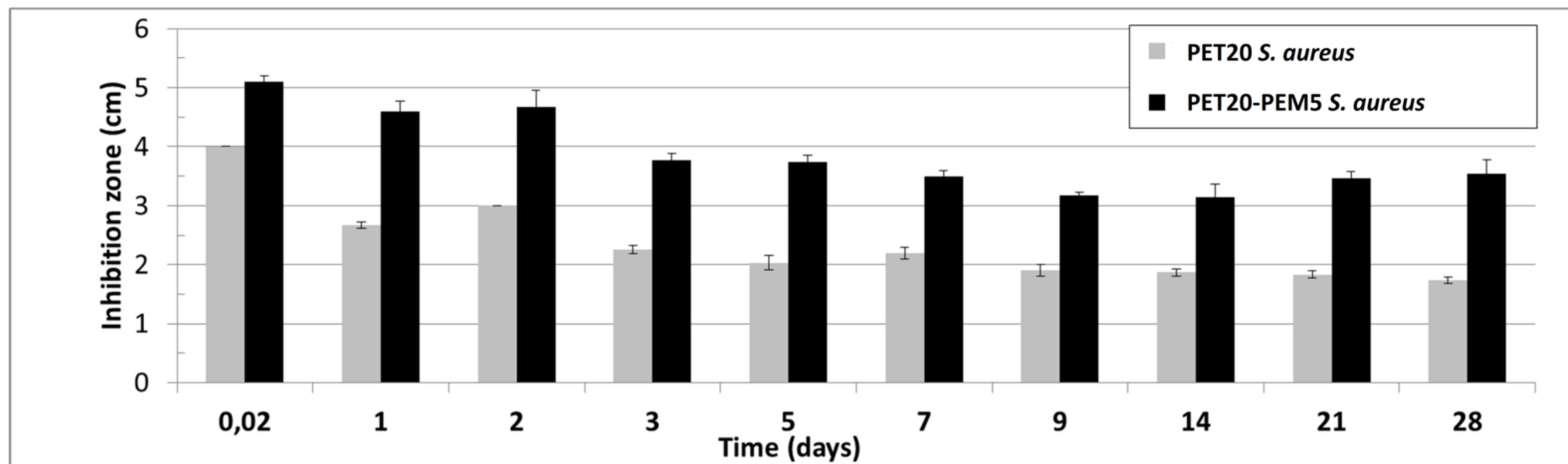
a

PET 20

PET20-PEM5

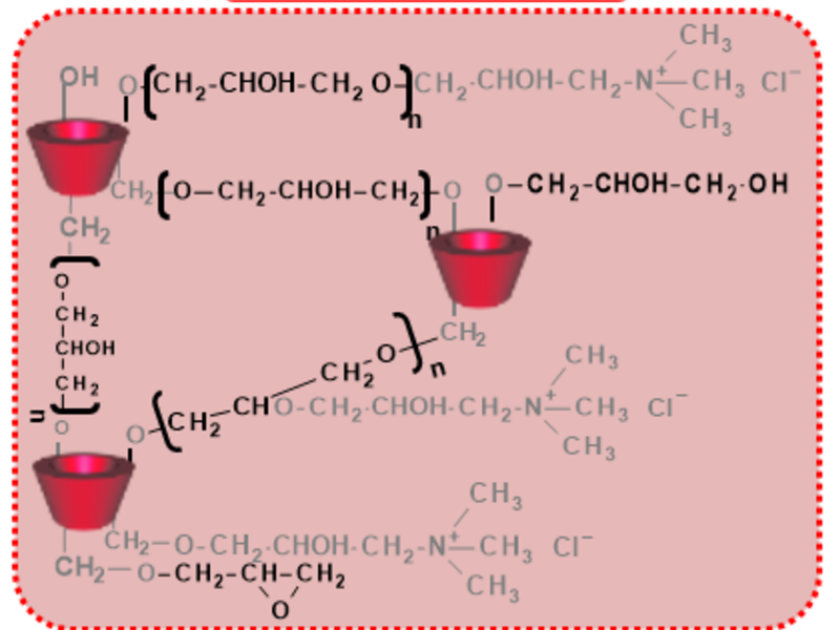


b

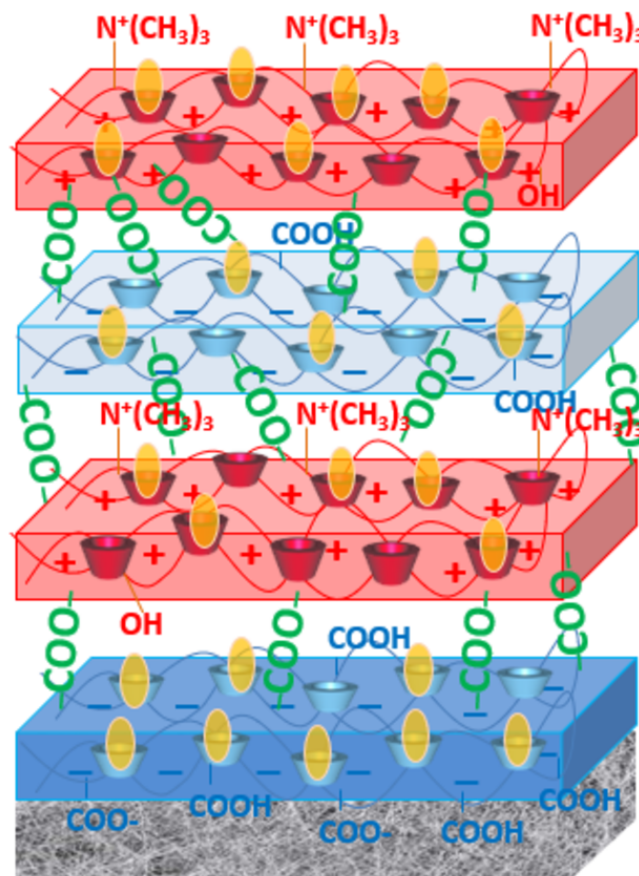
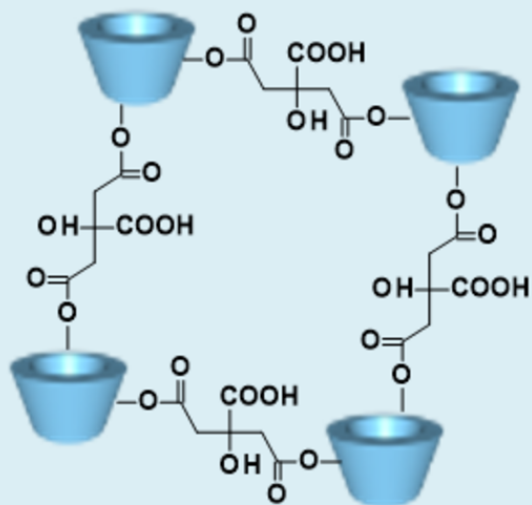


c

poly-EPG-CD-10 = PCD+



polyCTR-CD = PCD-



● Triclosan

Self assembled polyCTR-CD

Self assembled poly-EPG-CD-10

Ester link formed by post-treatment at 140°C

Nonwoven with thermofixed polyCTR-CD layer